1985

Fiber Optic Temperature Sensor for a Large Electric Power Generator

Daniel A. Lester
University of Central Florida

FIBER OPTIC TEMPERATURE SENSORS FOR A LARGE ELECTRIC POWER GENERATOR

BY

DANIAL A. LESTER
B.S.E., University of Central Florida, 1983

THESIS

Submitted in partial fulfillment of the requirements
for the degree of Master of Science in Engineering
in the Graduate Studies Program
of the College of Engineering
University of Central Florida
Orlando, Florida

Fall Term
1985

ABSTRACT

Fiber optic temperature sensors are excellent candidates for monitoring the temperature along the stator windings of a large electric power generator. Unlike thermocouple thermometers, they are immune to the effects of strong magnetic fields which are present in all power generators. Several different point and line sensors have been evaluated in their ability to resolve temperature and temperature distribution (respectively), as well as their compatibility with the generator environment. The sensor must function inside the generator for long periods of time (up to 25 years) without benefit of recalibration. This constraint has required us to devise methods by which the sensor may remain permanently calibrated. In almost all cases, it is necessary to measure a natural characteristic of a device which is temperature sensitive in order to achieve permanent calibration. This will enable the device to function despite the varying characteristics of the source and detector equipment.

ACKNOWLEDGEMENTS

I would like to express my gratitude to my parents for their emotional and financial support.

Also, many thanks to Dr. Roy Walters for his patience and guidance throughout this project.

Sincere appreciation goes to Michael Tracy and my brother, Kenny, for the use of their special facilities.

Westinghouse Inc. is to be thanked for their support of a task which is mutually beneficial to industry and academia.

TABLE OF CONTENTS

LIST OF ILLUSTRATIONS

LIST OF TABLES

CHAPTER 1

INTRODUCTION

Optical fiber temperature sensors are a viable alternative to thermocouple thermometers in many situations. While thermocouples will fail under exposure to large magnetic fields; the light within a fiber is relatively immune to such external fields. The magnetic fields present within large electric power generators and a requirement to measure temperature in the stator runs is the provided motivation for this research effort.

There are several different measurement concepts related to optical fiber temperature sensors. These concepts can be categorized into three broad areas.

1. High resolution point sensor

The high resolution point sensor can only measure the <u>average</u> temperature over a small area. The main advantage of this type of sensor is that it can detect small changes in temperature quite accurately. The required sensitivity and dynamic range are important considerations in analyzing the applicability of point sensors.

2. Low resolution line sensors

In many cases, one wishes to determine what the temperature is everywhere along the length of a piece of

fiber. The typically lower resolution of line sensors may be acceptable if they can give a good description of the temperature distribution. This solution requires the use of a pulsing device such as an optical time domain reflector (OTDR) unit (see chapter 5).

3. Threshold line sensor

This method can be used to determine exactly where a point has risen above a certain temperature.

All of these concepts should be assessed as to their ability to relay information about a point (or region) that is physically separated from the light source and the detector equipment. The sensor(s) must also be allowed to remain in place and calibrated for long durations of time.

This leads us to the problem of obtaining a permanent calibration for the sensor. There are many types of sensors which require periodic recalibration for one reason or another. These are unacceptable for many applications. In general, it is easier to obtain calibration by measuring a natural phenomenon (such as a shift in frequency), than by measuring a quantity whose source may not be constant (such as intensity).

Also, there are two basic methods by which the fiber(s) are used to relay temperature information. One uses the fiber only to communicate light information to and from a temperature sensitive optical material. The other method involves using the mechanical properties of the fiber itself

to determine temperature. We have constructed sensors based upon both of these methods.

The thin film interference filter temperature sensor is a good example of a point sensor which uses the optical fibers only to guide light to and from the device. The light source may be either narrow band (within the transmission band of the filter) or broad band with an effectively constant power spectrum over the filter's region of transmission. We performed experiments using both of these types of sources. The fraction of the narrow band source intensity transmitted by the filter was found to be a nearly linear function of temperature over the temperature region 20°C - 100°C. However, it is difficult to maintain the calibration of a sensor based upon intensity. In this case, the feed and read fibers' transmission characteristics will change with both temperature and ageing. Also, whenever the source or detector is replaced due to failure, the replacements may not have the same output or detectivity (respectively) as the originals. Thus, the narrow band source transmission sensor cannot be permanently calibrated.

When a broad band light source was used, the output power spectrum was the input power spectrum multiplied by the filter's power transmission spectrum (which changed as a function of temperature). The output was sampled by a spectometer in order to obtain the average value of the wavelengths transmitted by the filter. Since the spectrum

is not dependent upon the source's intensity or the transmittance of the input and output fibers, permanent calibration is obtained with this sensor. The fibers must remain at a constant angle to the filter surface as its transmission spectrum is dependent upon the angle at which light enters the device.

Interferometric sensors use the phase change due to fiber expansion to measure temperature. While they are extremely sensitive to temperature changes, they are also very sensitive to external vibrations. This made the interferometer difficult to build and maintain in a laboratory environment. Therefore, it is not a good candidate for a sensor which must operate in a rugged environment (such as an electric power generator).

The attenuation of power within an optical fiber and the number of spatial modes which are allowed to propogate down the fiber are also functions of temperature (due to a temperature dependence of the fiber's numerical aperture). While it is important to know the transmission characteristics of the optical fibers which are used in a sensor system, these characteristics alone do not generally provide enough resolution or consistency to base a temperature sensor upon them.

There are methods by which these fiber characteristics may be used to form a threshold distributed (line) sensor. A threshold line sensor can detect a "hot spot" along the

stator runs of a generator. An OTDR can be used to determine where the hot spot is located. For a practical temperature measurement system operating with a large electric power generator, a combination of these techniques will be required in order to relay information about the magnitude and distribution of temperature at critical points along the stator runs.

CHAPTER 2

TEMPERATURE MEASUREMENT USING A THIN FILM INTERFERENCE FILTER

Section 2.1: Introduction

One method of remote temperature measurement involves using optical fibers to read the transmission spectrum of a thin film interference filter which is sensitive to temperature due to the thermal expansion and/or changes in the refractive index of the film layers. An optical fiber is used to transmit light to the remote filter and back to the detectors and signal processing equipment. This is shown in Figure 2-1. The lead-in and lead-out fibers are assumed not to be sensitive to temperature changes with respect to the filter's change in spectral transmission.

Section 2.2: Fabry-Perot Cavity Theory

In order to understand the principle upon which this device operates, one must first understand the theory behind

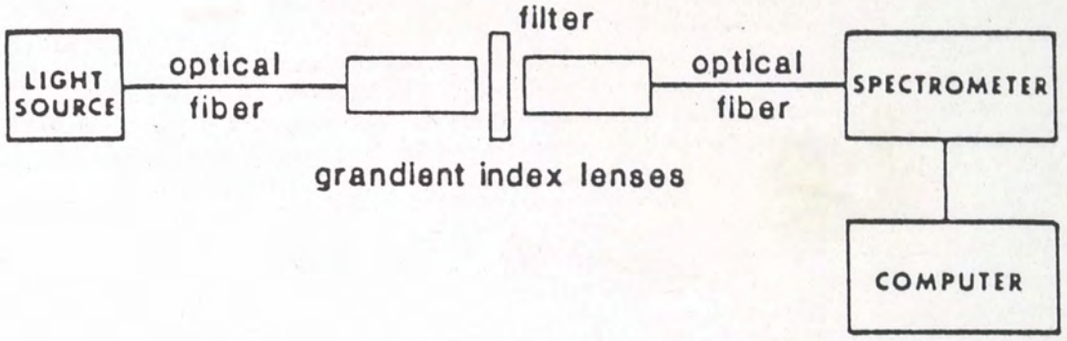

Figure 2-1. Filter Transmission Temperature Sensor.

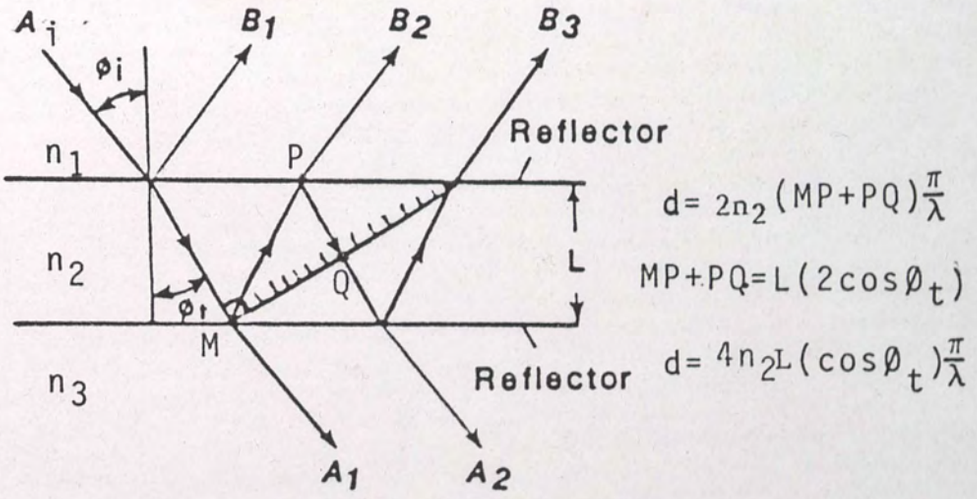

Figure 2-2. Fabry-Perot Cavity Diagram.

Source: see End Note 1.

the Fabry-Perot interferometer. We will examine the case of light from a plane wave incident upon a planar, parallel plate (at angle $\emptyset_i$ to the normal), of thickness L and index of refraction n_2 sandwiched in between mediums with indices n_1 and n_3. This is shown in Figure 2-2. For simplicity, we will initially assume that the media n_1 and n_3 are infinite in thickness.

We can treat the transmission (or reflection) of the plane wave through medium 2 by considering the infinite number of rays (partial waves) produced by reflections at the two end surfaces. The phase delay "d" between the n_2-n_3 boundary and the point where the reflected ray intersects that phase front again, (using Figure 2-2) can be shown to be:

$$d = (4\pi n_2 L\cos\emptyset_t)/\lambda \qquad [2\text{-}1]$$

where λ is the free space wavelength of the incident wave and $\emptyset_t$ is the angle of incidence within medium 2. If the incident wave is assumed to be a reference wave (i.e. it has a relative phase of zero in the expression for wave propagation), then

$$\begin{aligned} A_1 &= tt'A_i \\ A_2 &= tt'rpA_ie^{id} \\ A_3 &= tt'r^2p^2A_ie^{i2d} \quad . \; . \; . \end{aligned} \qquad [2\text{-}2]$$

where r is the reflectivity for a wave in medium 2 incident upon medium 3, p is the reflectivity for a wave travelling

in medium 2 incident upon medium 1, t is the transmissivity from medium 1 to medium 2 and t' is the transmissivity from medium 2 to medium 3. Also, a constant phase factor corresponding to the delay between the two surfaces has been left out. The complex amplitude of the transmitted wave is given by A_t where $A_t = A_1 + A_2 + A_3 + \ldots$ or using equation [2-2] we may put this in the form[1]

$$A_t = A_i tt'(1 + rpe^{id} + r^2p^2e^{2id} + r^3p^3e^{3id} + \ldots) \qquad [2\text{-}3]$$

this infinite series may be evaluated by considering that

$$(1 - a)(1 + a + a^2 + a^3 + \ldots a^n) = (1 - a^{n+1})$$

as n approaches infinity, a^{n+1} approaches zero for[2] $a < 1$. Thus we may rewrite equation [2-3] as

$$A_t = A_i tt'/[1 - (rp)e^{(id)}] \qquad [2\text{-}4]$$

A similar expression may be derived for reflection.

If our temperature measurement device has light at normal incidence ($\emptyset_i$=0) to the filter, we may reduce equation [2-1] to:

$$d = 4\pi n_2 L/\lambda \qquad [2\text{-}5]$$

In most real detection systems, the average output power (EE*) is the measured quantity (as opposed to the electric field). Equation [2-4] may be altered easily to take this into account.

$$\frac{p_t}{p_i} = \frac{A_t A_t^*}{Ai^2} = \frac{(tt')^2}{1 + r^2p^2 - (2rp)\cos(d)} \qquad [2\text{-}6]$$

reducing, this becomes:

$$\frac{p_t}{p_i} = \frac{A_t A_t^*}{A_i^2} = \frac{(tt')^2}{(1-rp)^2 + (4rp)\sin^2(d/2)}$$

where d is defined by eqn[2-1]. [2-6a]

Consider now an alternate arrangement to the setup shown in Figure 2-2. This is shown in Figure 2-3.

The partial mirrors both have reflectivity r. If L is on the order of λ, then the separation of the transmission wavelengths will be wide. The block filters will not transmit any other fringes[3] as is evident in Figure 2-4 (a), (b), and (c). Figure 2-4 (a) shows typical transmission characteristics for several values of R. Figure 2-4 (a) is a plot of equation [2-6] with $t = t'$ and $r^2 = p^2 = R$. The block filters are chosen so as to only transmit a certain range of wavelengths. The Fabry-Perot arrangement further narrows the transmission spectrum between the blocked wavelengths. Let us use an example to help to illustrate this procedure.

If high pass and low pass block filters are placed on top of each other, the lump transmittance of the two filters is pictured in figure 2-4 (d).

Using the configuration of Figure 2-3, with $n_2 = 1.5$ and $R = .87$, we shall design a Fabry-Perot cavity which will have its maximum transmittance at $\lambda = 633$nm, while

passing no other bands. Also, we shall specify the full width half power bandwidth around the peak wavelength.

Solution: From equation [2.6a],

$$\frac{P_t}{Pi} = \frac{(1 - R)^2}{(1 - R)^2 + 4R\sin^2(d/2)} \qquad [2\text{-}7]$$

We see that the argument (d/2) must be equal to $m\pi$ at $\lambda = 633$ nm. (Where m is an integer) From Figure (2.4) we see that the pass bands are very narrow; hence the peaks from m - 1^{th} band and the m + 1^{th} band must be outside of the absorbing filter's transmission spectrum. From these assumptions we may write the inequalities

$$(m - 1)(750nm) \leq 2n_2L \qquad \text{and}$$

$$(m + 1)(500nm) \geq 2n_2L$$

also, knowing that

$$m = 3L/633 \times 10^{-9} \quad (L \text{ in meters})$$

We may solve for the constraints above to find that (m) must be less than 3.66. Since m is necessarily an integer, we now know that m = 3 is the best choice. This yields a value of L = 633nm.

In practice, a combination of thin films with different indices are placed between the partial mirrors. These are also used in connection with the absorbing filter. For a thorough treatment of multilayer cavities, the reader is directed to Born and Wolf (1965)[4].

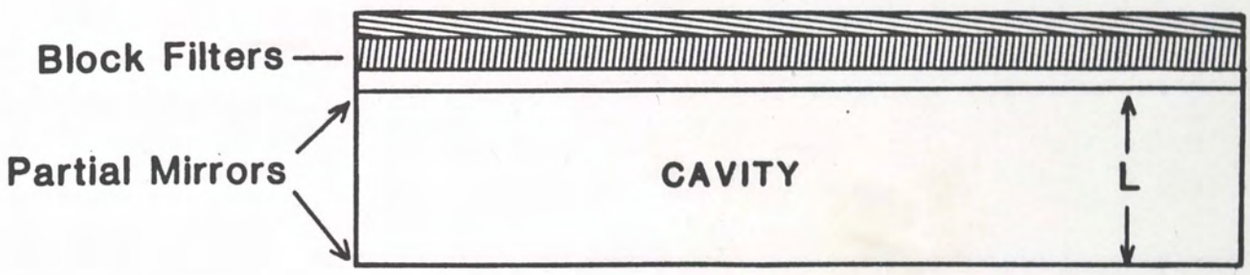

Figure 2-3. Fabry-Perot Cavity With Block Filters.

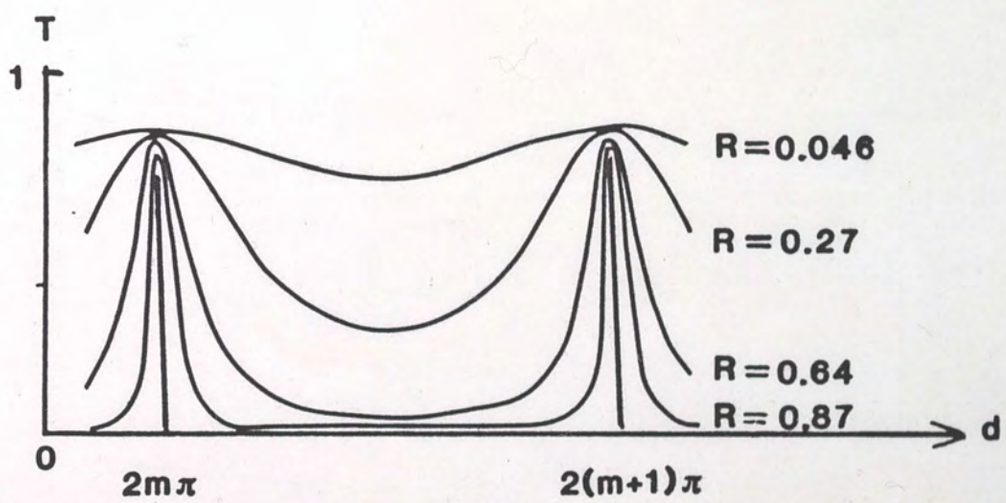

Figure 2-4 (a). Transmittance vs. Cavity Length for Several Values of Mirror Reflectance.

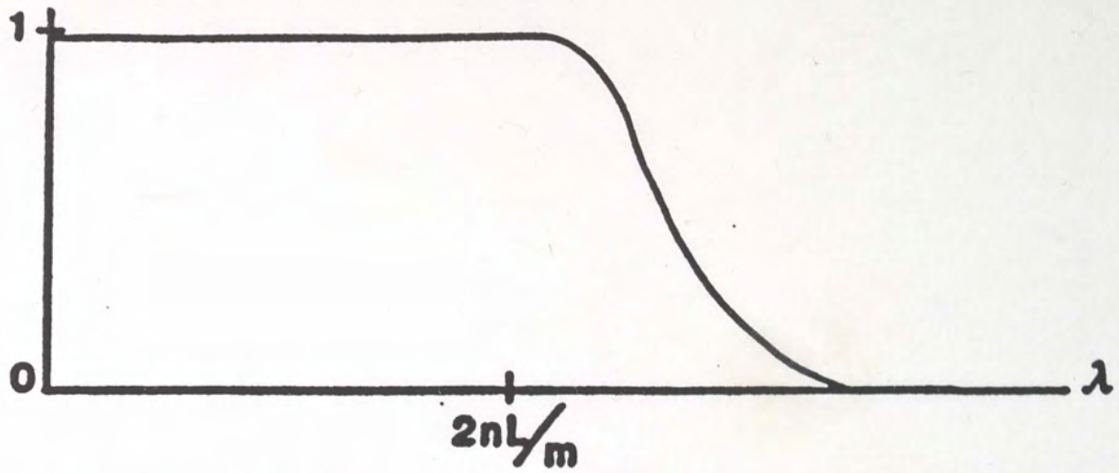

Figure 2-4 (b). Low Pass Filter Characteristics.

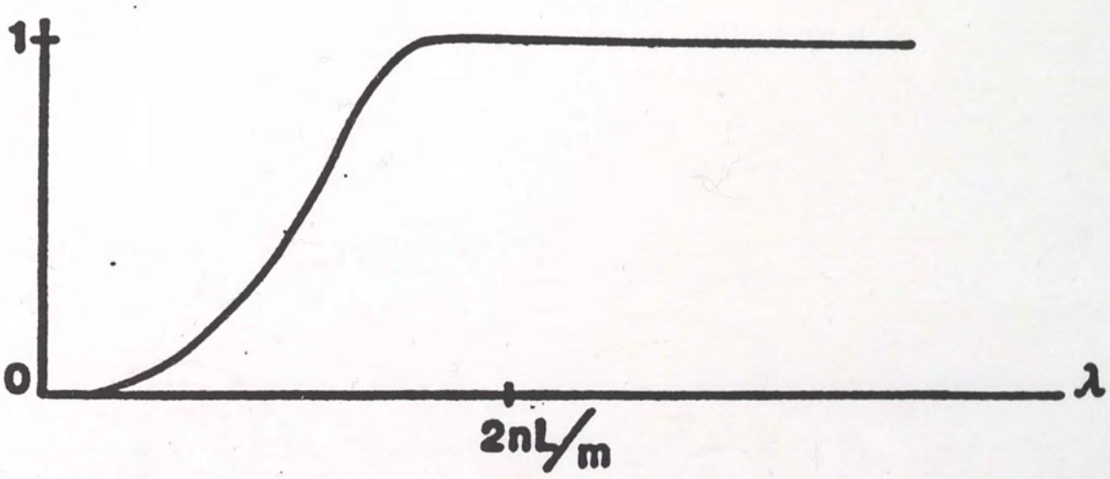

Figure 2-4 (c). High Pass Filter Characteristics.

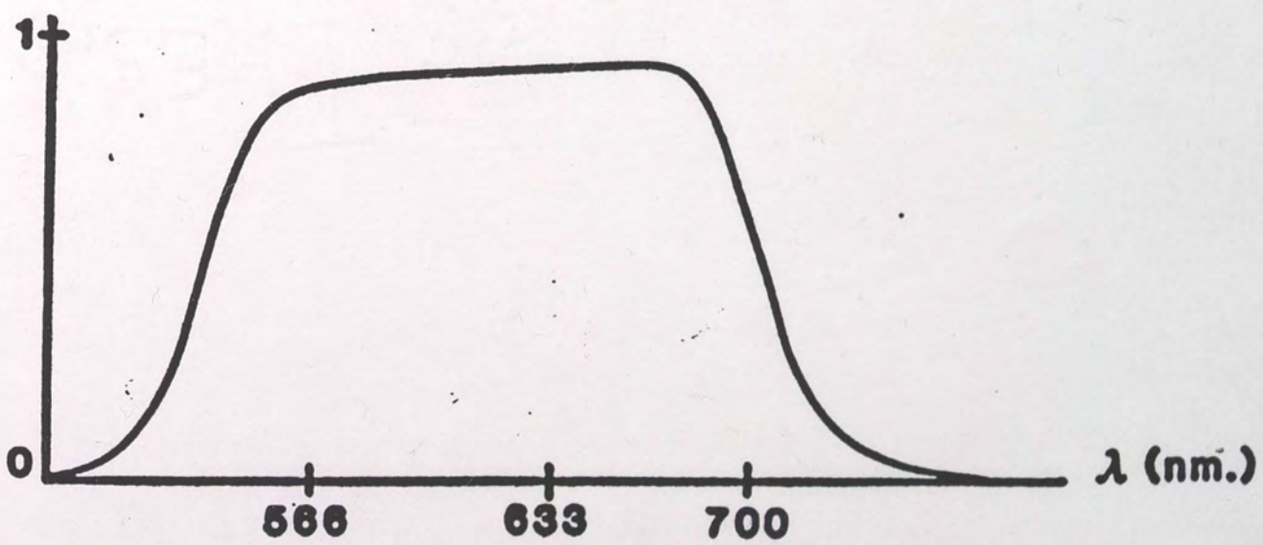

Figure 2-4 (d). Lump Filter Transmittance.

Section 2.3 Effects of Temperature Upon Thin Film Interference Filters

Like all materials, the characteristics of the films in an interference filter will change with an increase in temperature. One can see from equation [2-5] that as L or n_2 changes with temperature, the transmitted power at a given wavelength within the pass band of the cavity will also change. In general, the transmission spectrum within the pass band will shift toward longer wavelengths as a function of temperature.

A typical film layer will have a value of $2X10^{-5}/°C$ for its thermal coefficient of expansion.[5] This coefficient describes the differential increase in length with temperature.

The index of refraction n_2 is also a funtion of temperature. A typical value of dn_2/dT (for $n_2 = 1.5$)[6] will be $-10^{-5}/°C$. In general, the filter manufacturer will select his films so as to minimize the lump effects of temperature upon L and n_2 and therefore Pt/Pi. This may be illustrated by a differential analysis of the argument in equation [2-7] where d is defined by equation [2-1] to be equal to $4\pi n_2 L\cos\phi_t/\lambda$. If we consider a very slight change in n_2 of ϵ and a very small change in L of δ , then equation [2-7] becomes

$$\frac{Pt}{Pi} = \frac{(1-R)^2}{(1-R)^2 + 4R\sin^2[(2\pi(n_2 + \epsilon)(L+\delta)\cos\phi_t/\lambda]}$$

If we substitute our typical values for the thermally induced changes in n_2 and L for a change of 1°C (as well as the filter specifications derived in the example of Section 2.2), we obtain an increase in the argument d/2 of approximately $10^{-5}(d/2)$. Physically, this represents a positive increase in the wavelength of maximum transmittance of $10^{-5}\lambda$ or, for $\lambda = 633$nm., a change in wavelength of .0063nm/°C. Also, a change in temperature will result in a change in Pt/Pi at any given wavelength. If 6333.00nm is the peak wavelength of transmission (i.e. Pt/Pi = 1) for our example filter, and the temperature increases 1°C, then Pt/Pi will decrease very slightly (on the order of 10^{-8}). For a change of 100°C, however, we have a change of 10^{-3} in Pt/Pi. Obviously, our filter will need to be more sensitive to temperature if we wish to determine the temperature from the value of Pt/Pi.

The value of reflectance (R) can also vary with temperature. If we take the first derivative of equation [2-7] with respect to R, we see that there is a positive increase in Pt/Pi for a decrease in R. This is also evident in Figure 2-4(a). This change in Pt/Pi is symmetric about the value of d which yields the peak transmission.

While this change in R may be catastrophic for a temperature sensor based upon the transmission of a monochromatic source through the filter (at least as far as the theory is concerned), the symmetric change in spectral

transmission will not show up in a sensing technique based upon spectral averaging because the changes are averaged out in the formulation of the average wavelength vs. temperature (see section 2.5) .

For typical filters, this will yield a wavelength shift of the spectrum in the range of .005 to .03 nanometers per degree centigrade.[7] Figure 2-5 shows a Corion Optical filter's specifications. Unlike the filter described in the example, however, there are no block filters attached to the cavity. This will allow the $m + 1^{th}$ and $m - 1^{th}$ bands to pass (and other order bands also should the source be broad enough). As stated in the specification sheet, the wavelength shift with temperature is .018nm/°C.

The filter takes a finite amount of time to respond to an increase (or decrease) in the ambient temperature. The temperature response with time may be modelled as a first order differential equation relating the filter's heat capacity and thermal conductance to the change in radiant energy incident upon the sensor. If the material must absorb H joules in order to be raised 1 degree Kelvin, then H is known as the heat capacity of the object. The amount of heat capacity per gram of material is known as the specific heat (C_p) so that $C_p m = H$. The thermal conductance of the material (k) is the amount of constant power required to keep the detector 1 degree Kelvin above ambient at

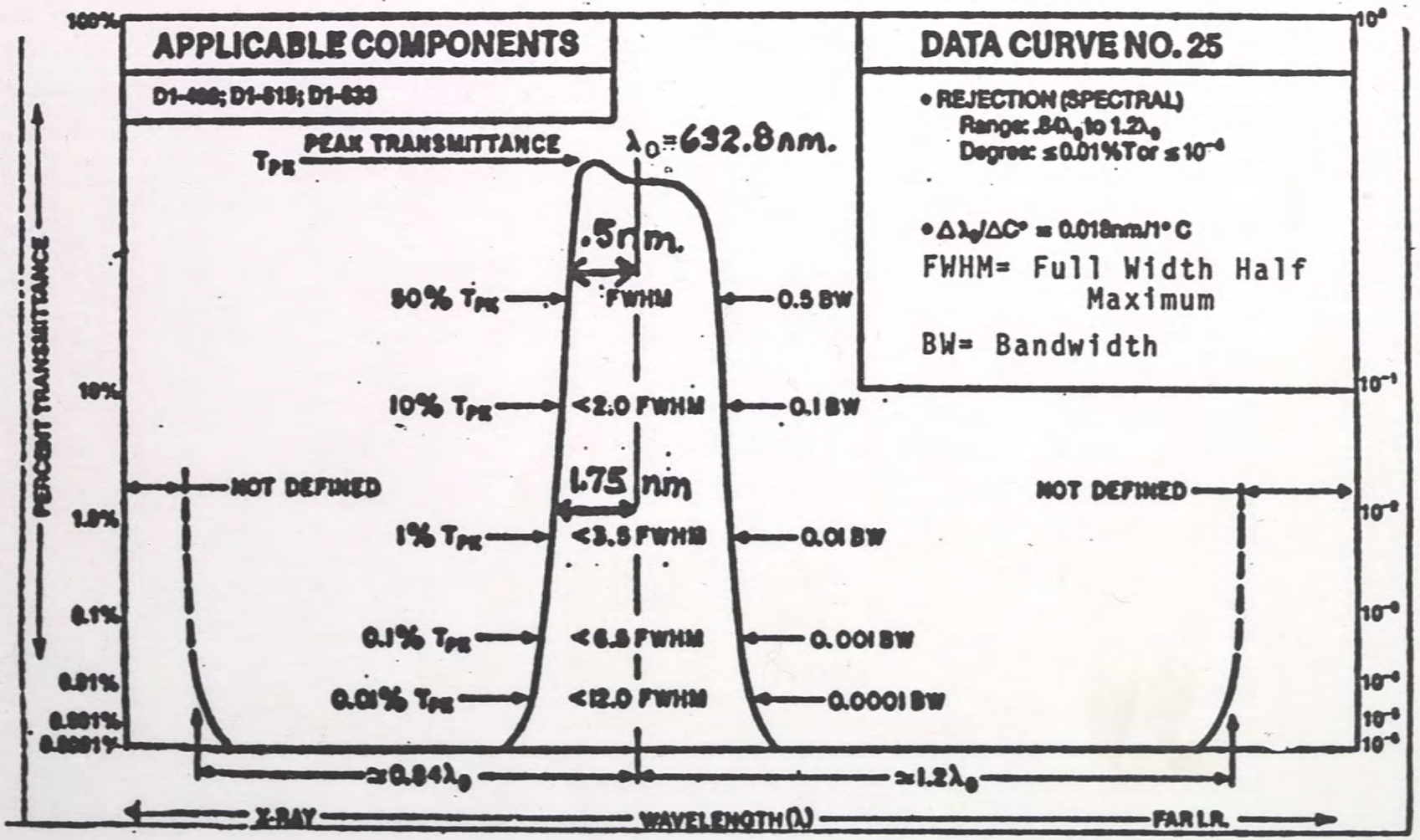

Figure 2-5. Corion #25 Data Curve.

Source: "Optical Filters and Coatings", Corion Corporation Catalog (Holliston, Mass. 1983) p. 44

equilibrium. The differential equation which describes the thermal response is equation [2-8]

$$H \frac{d(T_D - T_A)}{dt} + k(T_D - T_A) = aP \qquad [2\text{-}8]$$

where T_D is the temperature of the detector, T_A is the ambient temperature, a is the absorbitivity of the material and P is the radiant power incident upon the detector. The radiant power may itself be dependent upon the temperature difference; however, in most cases, equation [2-8] is an excellent approximation since an average power of $k(T_D - T_A)$ must be supplied to the material if it is to stay at T_D. The general solution to equation [2-8] is given by

$$(T_D - T_A) = (A)\exp[-Kt/H]$$

where t, of course, is in seconds.

If P is assumed to be a step at t = 0 with magnitude P_o, it is easily shown that the total solution of equation [2-8] is given below.[8]

$$(T_D - T_A) = (aP_o/H)\ [1-\exp(-Kt/H)] \qquad [2\text{-}9]$$

Second order effects (such as thermal diffusion) may cause a slightly different response. There will be spatial as well as temporal fluctuations across the filter in these cases. This will cause the width of the films to vary somewhat while responding to a sudden temperature rise.

Glass typically has both a relatively small value of thermal conductance; as well as a relatively high specific heat. As evident from equation [2-9], these conditions will result in a slow response time for a large filter. In a temperature measurement system, the filter should ideally be fitted to the input and output fiber diameters. This will reduce the mass and therefore the heat capacity. The lower value of heat capacity will in turn, decrease the response time of the filter. Also, second and higher order effects are generally minimized by a smaller filter size.

Section 2.4: Temperature Measurement by Transmission of Narrow Band Light Source Through a Cavity Filter

As was shown in earlier sections, the transmission spectrum of the filter will shift towards longer wavelengths with an increase in temperature. As the filter expansion is linear with temperature, the spectral shift verses temperature is also linear. Consider the room temperature Corion filter spectrum shown in Figure 2-6. A narrow band source at 633 nm wavelength is highlighted. As the spectrum shifts with temperature, the percentage of input power transmitted by the filter also varied. The narrow band output intensity decreases with increasing temperature and increases with a decrease in temperature. It is best to

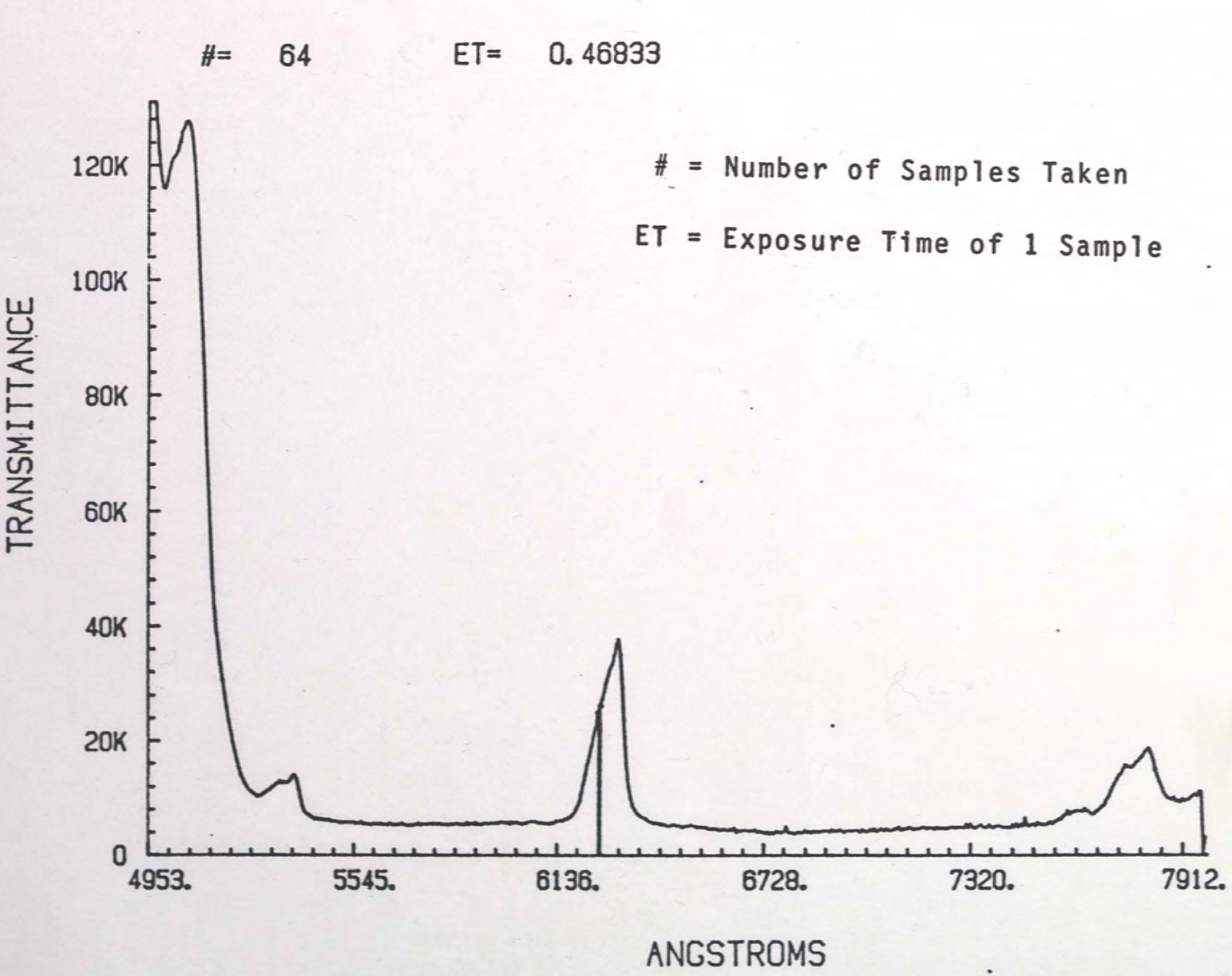

Figure 2-6. Room Temperature Transmittance vs. Wavelength of Corion #25 Optical Filter.

choose a source and filter combination which will allow the source to remain in the linear portion of the spectrum over the range of applicable temperatures.

Since this method is intensity-based, it is necessary to implement a differential detection amplifier. This will account for changes in source power output; as well as the replacement of connectors at the source or the detector end of the line. A plot of data obtained using the system in Figure 2-7 is shown in Figure 2-8.

The plot is nearly linear. Some variations from such are caused by the slight curvature of the spectrum. At some points, there are jagged edges. These are caused by the multi-film structure of the filter. The transmittance increases with decreasing temperature since 633 nm is on the lower wavelength part of the filter.

Section 2.5: Temperature Measurement by Spectral Shift

The spectral shift of the filter may be observed with a high resolution spectrometer. This shift can be measured quite easily. Even though the spectrometer may not have adequate resolution to closely track the peak, the average value of wavelength will encounter a measurable shift. The

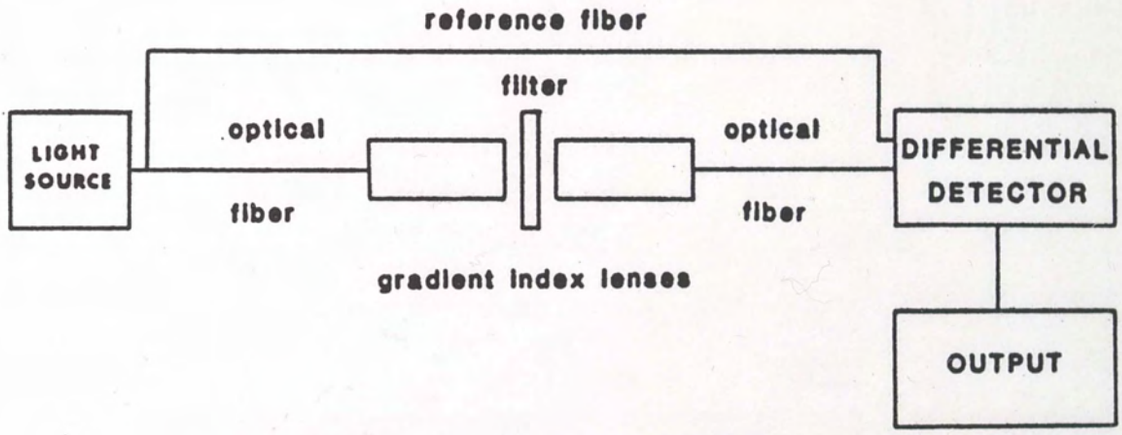

FIGURE 2-7. Transmission Temperature Sensor.

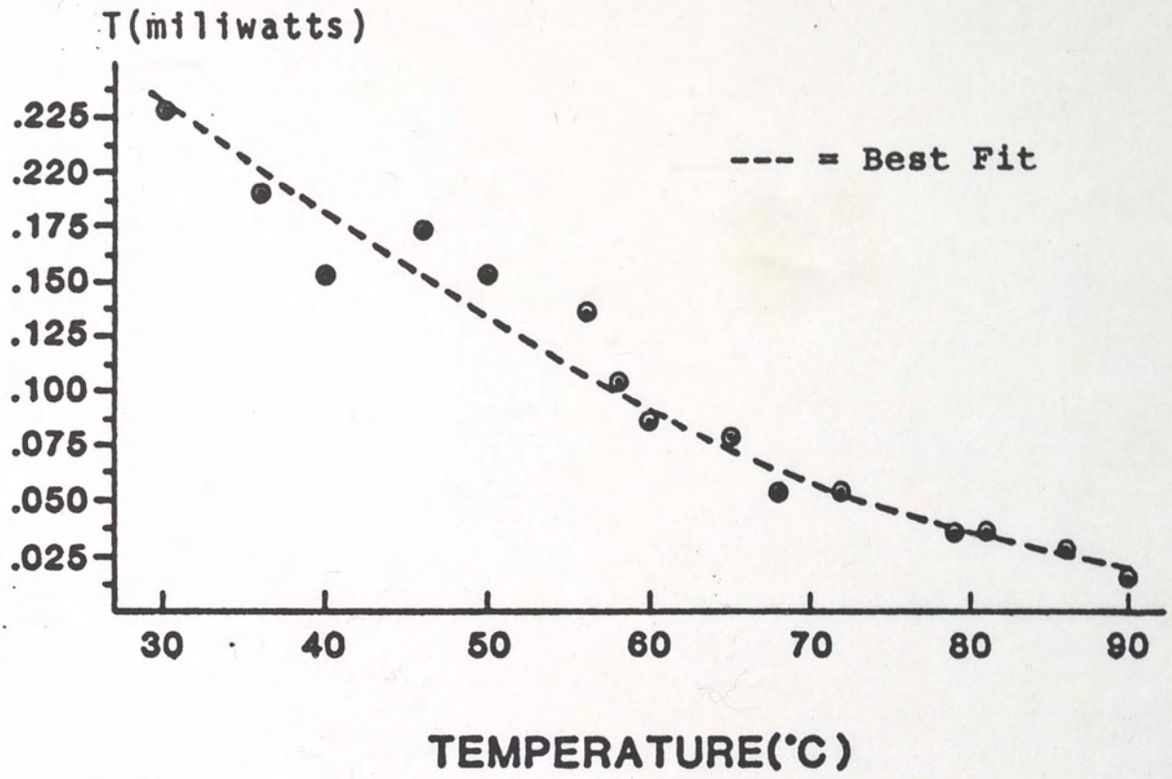

Figure 2-8. Transmission vs. Temperature, Corion # 25.

average wavelength can be calculated using the simple statistical formula:

$$\bar{\lambda} = \frac{\Sigma \lambda I(\lambda)}{\Sigma I(\lambda)} \qquad [2\text{-}10]$$

summed over the data points obtained from a spectral scan of the filter's transmission spectrum. A plot of average wavelength will increase linearly with increasing temperature. A plot of average wavelength verses temperature using the device shown in Figure 2-1 for a yellow-green filter is shown in Figure 2-9. If the spectrometer is computer compatible, a program may be designed which will control the spectrometer as well as process the data according to equation [2-10]. An example of a BASIC program which will control a Tracor Northern TN 1710-21 optical spectrometer via a GPIB (General Purpose Information Bus) is shown in the Appendix. One can see from Figure 2-9 that the plot is not exactly linear. For this filter, a linear regression of the curve will result in a maximum error of $\pm$ 3°C at any given temperature. Also, the data shows a mean error of less than 1°C. If more accuracy is required, the computer may be programmed to fit the curve in sections or by second order or higher order equations.

A source of possible error comes from the shifting of the filter angularly with respect to the source fiber. Any holder for the filter (and fibers) must remain extremely

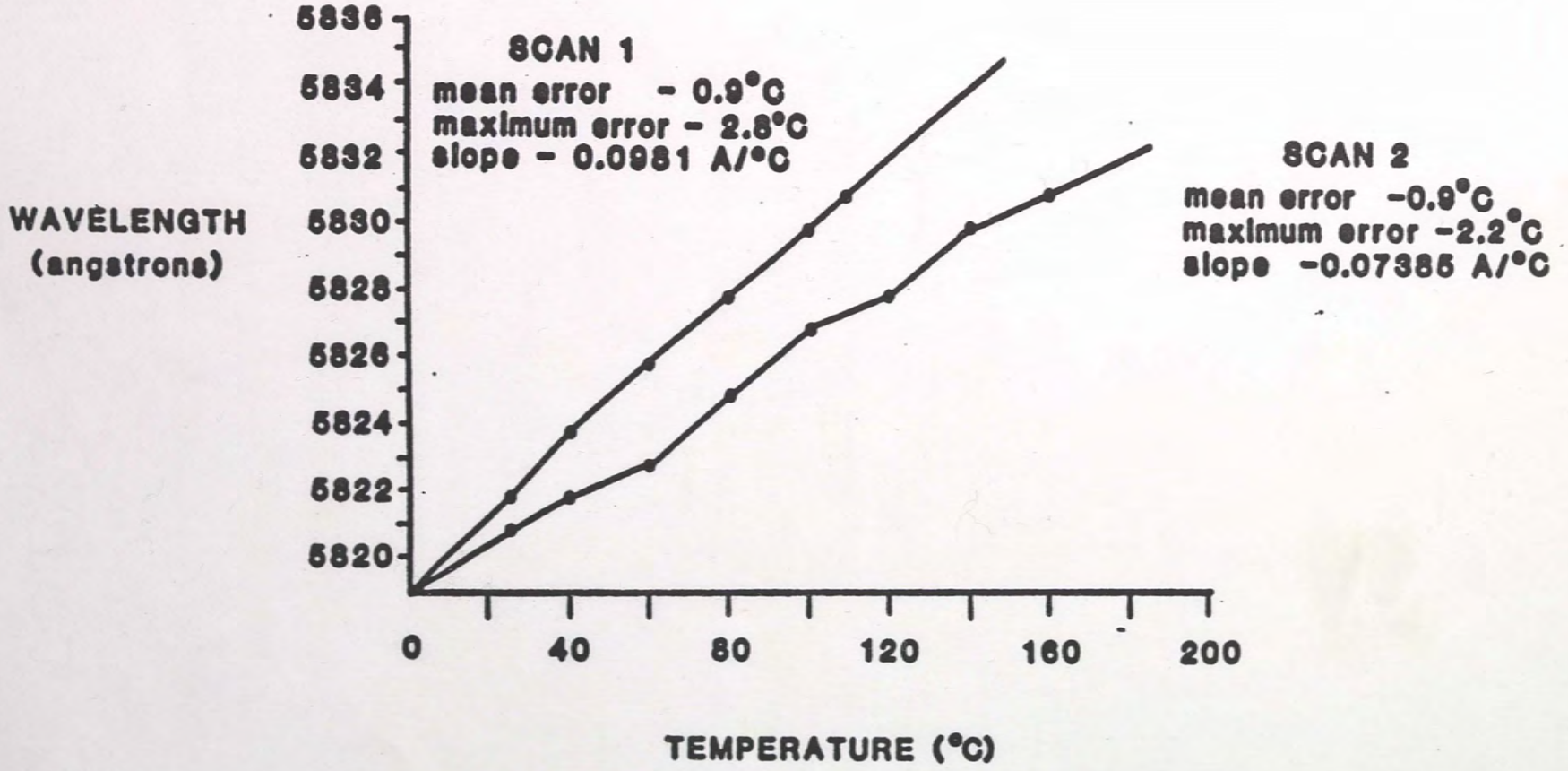

Figure 2-9. Average Wavelength vs. Temperature.

stable over a broad range of temperatures as it only takes a very small angle change to cause large spectral shifts (compared to the wavelength change due to filter expansion). This problem is evident from the two different scans shown in Figure 2-9.

In review, a practical system for measurement of temperature by monitoring the special shift of a Fabry-Perot Bandpass filter can be obtained via transmission or reflection techniques and by the use of a high transmission prism or grating spectrometer. It is expected that barring S/N problems, the relative spectral transmission of the system is independent of the source power.

CHAPTER 3

INTERFOMETRIC TEMPERATURE SENSORS

Section 3.1: Introduction

Interferometry is a method of length measurement where the fields from two mutually coherent beams are summed. For our purposes, only single-mode fibers can be used to guide the coherent light. The actual temperature sensing is derived from the phase difference between the beams of light in two fibers. The phase difference may be altered by changes in the length of one fiber with respect to the other, or relative changes in the core index of refraction. Both length and refractive index are functions of temperature. A diagram of an interferometer is shown in Figure [3-1]. Since the wavelength of light is so small, the fiber must change only a minute amount in order to cause a 2π radian phase shift in the output. For this reason, interferometry is extremely sensitive. When the output shifts 2π radians, the information about the absolute temperature position is lost. Although there are recovery methods which can overcome this problem, interferometric sensors in general have very low dynamic range. In addition

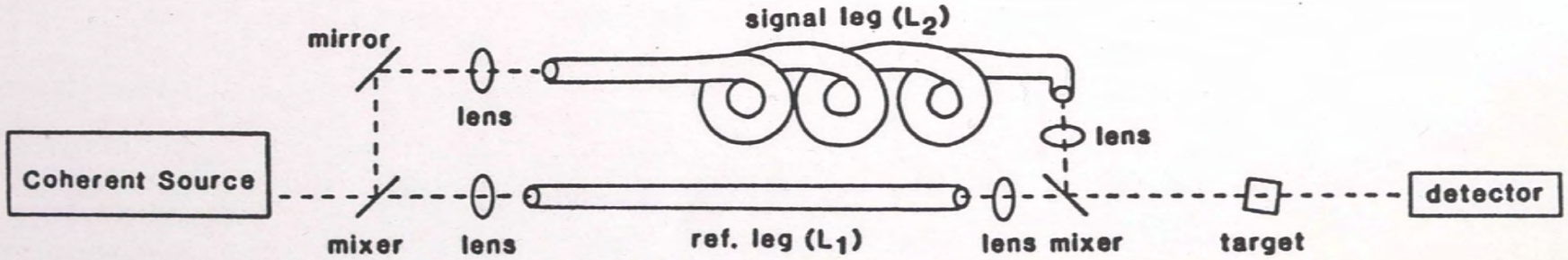

FIGURE 3-1. Interferometric Temperature Sensor Configuration.

to temperature sensitivity, interferometers are also very susceptible to mechanical vibrations. The actual single-mode fiber should be well protected from external perturbations other than those to be measured.

Section 3.2: The Mathematical Theory Of Interferometry

In order to perform interferometric measurements, it is necessary to use single-mode fiber. In order to be single mode at any given wavelength (λ), the fiber must satisfy the constraint[9]

$$(2\pi a/\lambda)\sqrt{n_1^2 - n_2^2} < 2.405 \qquad [3\text{-}1]$$

Where λ is the freespace wavelength, a is the core radius, n_1 and n_2 are the core and clad refractive indices respectively. The significance of the number 2.405 on the right side of the equation [3-1] is that it is the first root of the zeroth order Bessel function of the first kind. (Bessel functions are a common set of functions used in modelling modes in step index fibers.) The expression on the left of equation [3-1] is also known as the V number (V#) of the fiber.

For a V# less than 2.405, the phase front of the fiber output will be due to only one propagating spatial mode and is approximately planar. If the V# should be greater than 2.405, the phase front will be constructed of more than one

mode, with the various modes interfering with each other. This makes interferometric signal recovery difficult.

The output of a single-mode fiber can be modelled as a plane wave

$$E_1 = (A)\ \exp[i(wt - kz_1 + \emptyset_1] \qquad [3\text{-}2]$$

E_1 is the electric field output of the reference fiber. When two beams are mixed on a beam mixer, their electric fields are summed. Now, suppose we mix the beam in equation [3-2] with a beam of the form

$$E_2 = (B)\exp[i(wt - kz_2 + \emptyset_2)] \qquad [3\text{-}3]$$

Let us assume (for convenience) that the fields of both beams are polarized in the same direction. The sum of the two beams is therefore (with $\emptyset_1$ arbitrarily set equal to zero)

$$E_1 + E_2 = (A)\exp[i(wt - kz_1] + (B)\exp(i(wt - Kz_2 + \emptyset_2) \qquad [3\text{-}4]$$

If $K(z_1-z_2)$ is a multiple of 2π, then the intensity of the mixed beam will be (with $\emptyset = \emptyset_1 - \emptyset_2$)

$$I = \left| E_1 + E_2 \right|^2 = A^2 + B^2 + AB\ [\exp(i\emptyset) + \exp(-i\emptyset)] \qquad [3\text{-}5]$$

or, since $\exp(ia) + \exp(-ia) = 2\cos(a)$,

$$I = A^2 + B^2 + 2AB\ \cos(\emptyset) \qquad [3\text{-}6]$$

The angle $\emptyset$ is a real function of temperature. If we make the signal leg (L_2), longer than the reference leg (L_1), the angle $\emptyset = \emptyset_1 - \emptyset_2$ will change with index of refraction variations and elongation of the fiber in the form.[10]

$$\frac{\Delta\phi}{\Delta T} = \left[\frac{2\,n(L_1-L_2)}{\lambda}\right]\left[g + \frac{1}{n}\frac{dn}{dT}\right] \qquad [3\text{-}7]$$

where g is the longitudinal strain coefficient and $\frac{1}{n}\frac{dn}{dT}$ is the change in the refractive index of the core with temperature.

The sensitivity of the interferometer is described in units of radians/m°c or in fringes/m°c. Where

$$S_{(rad)} = \frac{\Delta\phi}{(L_1-L_2)\ T} = \frac{2\pi n}{\lambda} \cdot g + \frac{1}{n}\frac{dn}{dT} \qquad [3\text{-}8]$$

For a typical single mode fiber,

$$\frac{1}{n}\frac{dn}{dt} = -10^{-5} \quad \text{and } g = 5X10^{-7}\text{, and } n = 1.5$$

From equation [3-8], the sensitivity is seen to be

$$(-8.95X10^{-5}/\lambda)\ \frac{\text{radians}}{m°C}$$

For a λ of 632.8 nm. (from a Helium-Neon Laser) it is seen that $S_{(rad)} = -140$ rads/m°C. In many applications, the change in index with temperature is made much less negative by the addition of dopants[11] such as Neodynium. Also, the thermal expansion coefficient is made more positive by the introduction of impurities also resulting in a slightly increased index of refraction. Values for the parameters of the neodynium doped glass core fiber are

$$n = 1.52,\ \frac{1}{n}\frac{dn}{dT} = -4.5\ x10^{-6},\ g = 10^{-6}$$

Substituting these values into equation [3-8] yields $S = -52.8$ rads/m°c at $\lambda =$ 632.8 nm. A plot of the output of an interferometer with these characteristics around T =

50°C is shown in Figure 3-2. L_2-L_1 is assumed to be 1cm. Also, in equation [3-6] A = B, so the fiber output powers are equal.

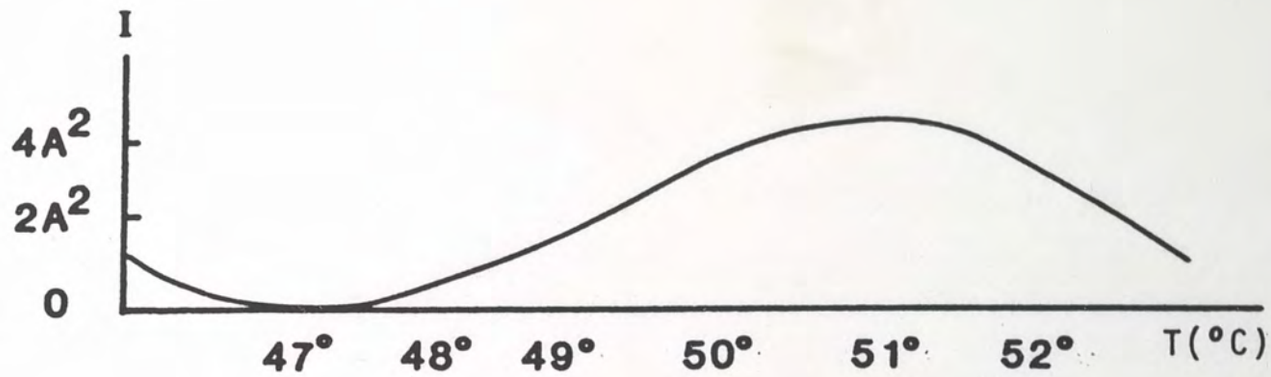

Figure 3-2: Interferometer Output Around T = 50°C

As one can see from the figure, the dynamic range of the interferometer is small. Over an 11 degree period, the interferometer will pass through a complete cycle. If a linear output, as a function of temperature, is desired, the range is only about 2°C. However, there are various signal recovery schemes which can track the periods of the interference thereby utilizing the sensitivity of this technique. With respect to practical termperature measurement (over a large dynamic range and in rugged environments), interferometry is not a consideration.

CHAPTER 4

EFFECTS OF TEMPERATURE UPON OPTICAL FIBERS

Section 4.1: Introduction

While measuring the transmission of light through an optical fiber as a function of temperature is a very simple sensor concept it has various drawbacks. The fiber may change over a period of time. Also, no two fibers (even from the same roll) are the same. This means that each fiber (sensor) must be calibrated individually and periodically.

Even though the transmission characteristics may not be a very reliable phenomenon upon which to base a sensor; it is still important to understand these characteristics for several reasons. Any remote sensor which requires lead-in and lead-out fibers to communicate with a temperature sensitive optical device must have fibers which are insensitive to temperature changes. Also, by using an optical time domain reflectometer (OTDR) unit (see Chapter 5), a good temperature sensor can be constructed based upon the backscatter of light which is dependent upon transmission. Almost all fiber sensors require a

fundamental knowledge of how temperature affects the basic transmission characteristics of the fiber.

Section 4.2: Fiber Temperature Measurement Through Escape of Higher Order Modes

The number of modes propagating in a multimode step index fiber asymtopically approaches the value

$$N \sim \left(\frac{2V}{\pi}\right)^2 \qquad [4\text{-}1]$$

rounded down to the nearest integer as shown in Figure 4-1. Where N is the number of modes propagating, and V is the "V" number of the fiber, which is defined as

$$V = K_c a = \frac{2\pi a}{\lambda}\sqrt{(n_1^2 - n_2^2)} \qquad n_2 < n_1 \qquad [4\text{-}2]$$

"a" is the fiber's core radius, λ is the free space wavelength of the source, n_1 and n_2 are the core and clad indices of refraction respectively. K_c is the cutoff spatial frequency of the guide.[12]

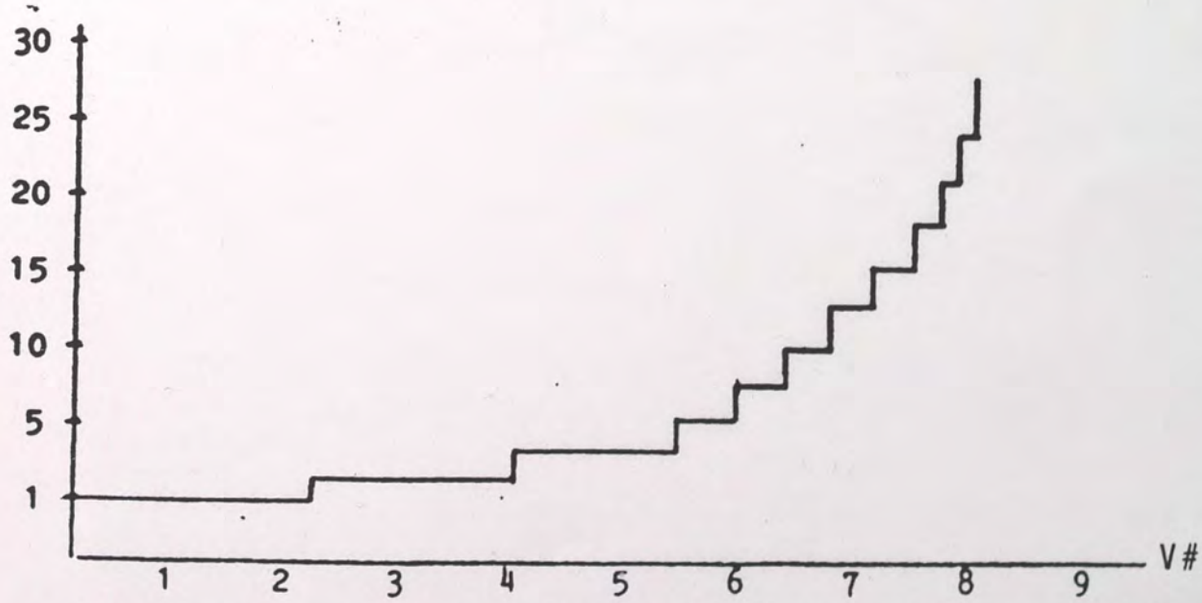

Figure 4-1. Number of Propagating Modes vs. Fiber V Number.

It is apparent from equations [4-1] and [4-2] that if the clad index of refraction (n_2) should decrease, the V number (and the number of propagating modes will increase). Physically this situation can be represented using a ray diagram as shown in Figure 4-2. The minimum angle at which a mode will escape from the guide is known as the angle of acceptance (Øacc).

Where

$$Øacc = \sin^{-1} [(n_1^2 - n_2^2)^{1/2}]$$

As n_2 increases, $n_1^2 - n_2^2$ decreases. Assuming that the numerical aperture $(n_1^2 - n_2^2)^{1/2}$ has the typical characteristic of being $<< 1$ then $\sin(Ø_{acc}) \simeq Ø_{acc}$.

If a constant light source is guided through a uniformly heated fiber, the (differential) intensity will be a function of the core and clad indices of refraction which which in turn are functions of the ambient temperature. Let us assume that we have a core which is made of a material relatively insensitive to temperature ($n_1 = 1.45$). Also let us assume that the clad refractive characteristics are shown in Table 4-1 and Figure 4-3.

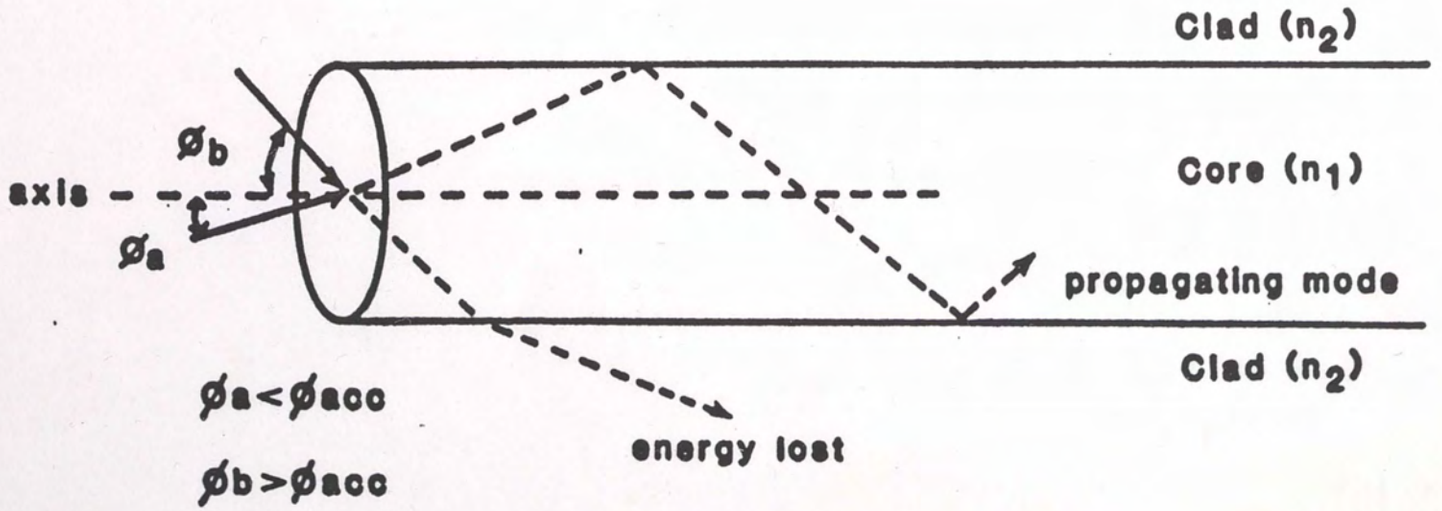

FIGURE 4-2. Optical Fiber Ray Diagram.

TABLE 4-1

THE MEASURED INDEX OF REFRACTION WITH TEMPERATURE

Temp (°C)	Index of Refraction
14.5	1.409
21.5	1.407
29.5	1.404
38.5	1.401

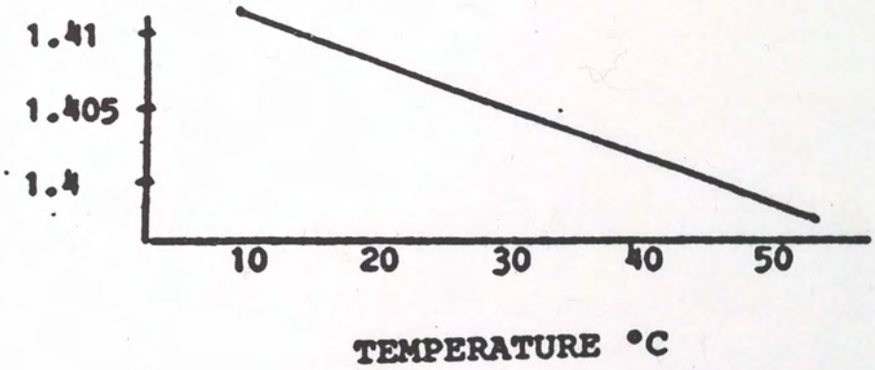

Figure 4-3. Measured Index of Refraction vs. Temperature for the Clad of a Fiberguide-100 Fiber.

Source: Fiberguide-100 Specification sheet.

Using the measured values of n_2 at various temperatures and equation [4-2] we obtain the values for V and N shown in Table 4-2 and Figure 4-4.

TABLE 4-2

NUMBER OF PROPAGATING MODES AT SEVERAL TEMPERATURES

Temp (°C)	V	N (Number of modes)	
			a = .05mm.
14.5°	170	11,700	
21.5	174	12,270	n_1 = 1.450
29.5	180	13,100	
38.5	185.6	13,950	λ = 632.8nm

In order to simplify our analysis of differential intensity change with temperature we assume that the total power output is directly proportional to the number of propogating modes. The consequence of using this assumption in conjunction with equation [4-1] is that all higher order modes are assumed to contain an equal amount of optical power. This is a reasonable assumption.

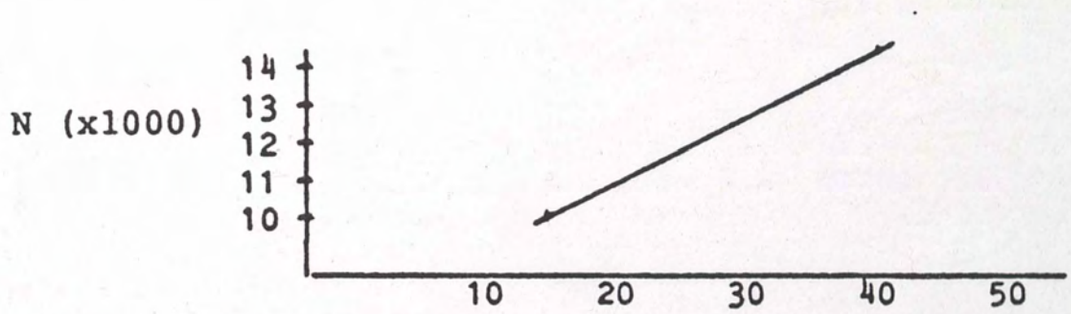

Figure 4-4.
Number of Propagating Modes vs. Temperature.

As one can see from Figure 4-4, there is approximately a linear relationship between temperature and the number of propagating modes.

The number of modes which will propagate in a multimode fiber as a function of temperature is shown in Figure 4-4.

From this data, the modal temperature dependence is seen to be approximately

$$\frac{\Delta N}{\Delta T} = 160 \text{ modes/°C}$$

and since intensity is defined to be proportional to N, the number of modes,

$$\frac{\Delta I}{I \Delta T} = \frac{\Delta N}{N \Delta T} \quad 1.23\%/°C \text{ for } N = 13{,}000$$

Note that this is a positive temperature coefficient. One is reminded that this is not a loss per unit length. It is a measure of the change of intensity over an undefined length that is supported by modal propagation. There is also a length dependence in that the fiber will now propogate more of the scattered light. Thus, one can also consider this as a decrease in attenuation.

One must provide a luminous intensity by which to measure the differential change in propagation with respect to temperature. Calibration is difficult since the source is not necessarily precisely regulated. Also, the amount of light which enters the guide is proportional to the coupling between source and fiber. The connection between fiber and detector is also important for similar reasons.

One method of differential measurement is to use a fiber which has a clad index of refraction sensitive to changes in temperature at one source wavelength, but which is relatively insensitive to changes in temperature at a second wavelength. This is as illustrated in Figure 4-5.

If we have a spectral source which has transitions at λ_1 and λ_2, we have an intensity at λ_2 which is less sensitive to temperature variations, and an intensity at λ_1 which is dependent upon temperature. The ratio $I(\lambda_1)/I(\lambda_2)$ is the parameter necessary to determine the temperature in the fiber. Since it may not be possible to obtain a fiber with the characteristics shown in Figure 4-5, a two fiber system including a signal fiber and a reference fiber may be needed.

A problem may arise in differential temperature measurements when the fiber at the source end is at a lower temperature than the fiber at the detector end. There are only a certain number of modes which will propagate through the colder part at the beginning of the fiber. The higher modes will have escaped before they arrive at the heated portion of the fiber. This is called mode stripping. Hence, there is no observable change in temperature. The best way to overcome this is to make a splice at the beginning of the heated area. This mixes the modes. In other words, the new boundary conditions alter the power distribution amongst the various modes.

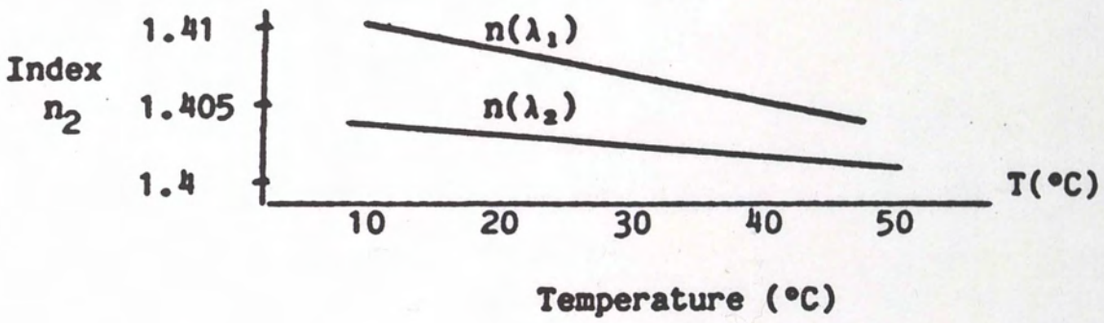

Figure 4-5. n_2 vs. T.

However, this is not the only problem with a temperature sensor based upon measuring the escape of higher order modes by measuring intensity. After mode mixing, the light at wavelength λ_2 may not escape to the clad as easily as the light at λ_1. The measuring device must be calibrated to accommodate the splice. Also, another splice can be inserted between the heated area and the detector end of the fiber, in order that the higher order modes (and thereby the temperature information) will not be lost should the fiber temperature near the detector be less than the temperature in the heated area. Modal propagation loss is of no concern in high loss fibers as attenuation is the dominant loss mechanism.

Section 4.3: Scattering Losses in Optical Fibers

In general, it is necessary to calibrate a measurement system to the length of fiber which is to be used to measure temperature. Each fiber has its own imperfections which may cause back scattering and/or mode mixing. Both of these effects will diminish the light intensity. Back scattering will do this by reflecting some of the light back at the source. Mode mixing will create higher order modes which will not propagate through the rest of the fiber. Actually, back scatter and mode mixing are both effects of scattering. The back scatter is the portion of the scattering (from an imperfection) which is reflected back toward the source.

The mode mixing comes from the light which is scattered in the forward direction at different angles. The scattering parameters depend upon the geometry of imperfections and the quality or bubble structure of the core.

If the fiber is long enough, the scattering due to imperfections in the fiber will become the dominant loss mechanism. There are two general types of imperfections in glass fibers. They are:

1. Intrinsic scattering
2. Concentration fluctuation scattering

1. Intrinsic Scattering

On the atomic level, the density (and therefore the index) of any transparent material is not constant due to thermal fluctuations. This is believed to cause the lower limit of attenuation in fibers. For a typical sample of pure fused silica; 820 nm light is lost at a rate of 1.7 dB/Km.[13]

2. Concentration Fluctuation Scattering

In many cases, a glass fiber core may be made of "doped silica." The dopants serve to change properties of the glass such as refractive index or the thermal expansion of coefficient. The presence of these impurities causes variation in refractive index throughout the fiber core. This causes loss due to scattering according to the expression.[14]

$$\alpha = \frac{16\pi^3 n}{3\lambda^4}\left[\frac{dn}{dC}\right]^2 \overline{(\Delta C)^2}\ \delta V \qquad [4\text{-}3]$$

Where $\overline{(\Delta C^2)}$ is the mean square impurity concentration fluctuation and δV is the differential volume over which it occurs. dn/dC is the index change with respect to concentration. There are other forms of scattering such as Raman and Brillouin scattering, but they make up only a small portion of the overall loss. However, they have properties which will change with temperature and may thus be observed by using an optical time domain reflectometer (OTDR).

Equation [4-3] above was developed assuming that all scattered light will be lost and the clad has a refractive index identical to that of the core. An optical waveguide does not have a core and clad with identical indices of refraction, although many have a lossy clad or jacket.

Since the core and clad have different refractive indices, not all of the scattered light will be lost to the clad. Rays which meet the criterion

$$|\phi_i| > \sin^{-1}\left(\frac{n_2}{n_1}\right)$$

will be totally internally reflected and will therefore only have an evanescent wave in the clad. As long as the clad is thick compared to the core and not lossy compared to the

core, the loss in the clad is negligible since the evanescent field is attenuated.

Since the concentration fluctuations are randomly oriented and positioned within the core, a ray incident upon them will be partially refracted to angle Øs which is uniformly distributed between

$$0 \leq \left|\emptyset_s\right| \leq \pi/2$$

Also, part of the ray will be reflected. The reflected ray Ør may be at any angle uniformly distributed between - and Figure 4-6 is split into two areas, "a" and "b," area "a" depicts a ray which is partially transmitted by the impurity concentration and partially reflected. The transmitted ray approaches the normal of the core clad interface at angle Øs $\sin^{-1}(n_2/n_1)$ and hence it is still guided by the fiber. Area "b" shows the incident ray striking on an impurity concentration at an angle Øi such that the transmitted ray is incident upon the core-clad interface at an angle Øs $\sin^{-1}(n_2/n_1)$. It therefore has a component which propagates in the clad and may be lost. Even though the ray is at an angle greater than $\sin^{-1}(n_2/n_1)$, a portion is reflected back into the core, however; each time it strikes another interface a portion will be lost again to the clad. If the reflectance of a ray striking the interface is R, then the percentage of the power in that ray remaining after the m^{th} reflection is given by:

$$P/P_i = R^m \qquad [4\text{-}4]$$

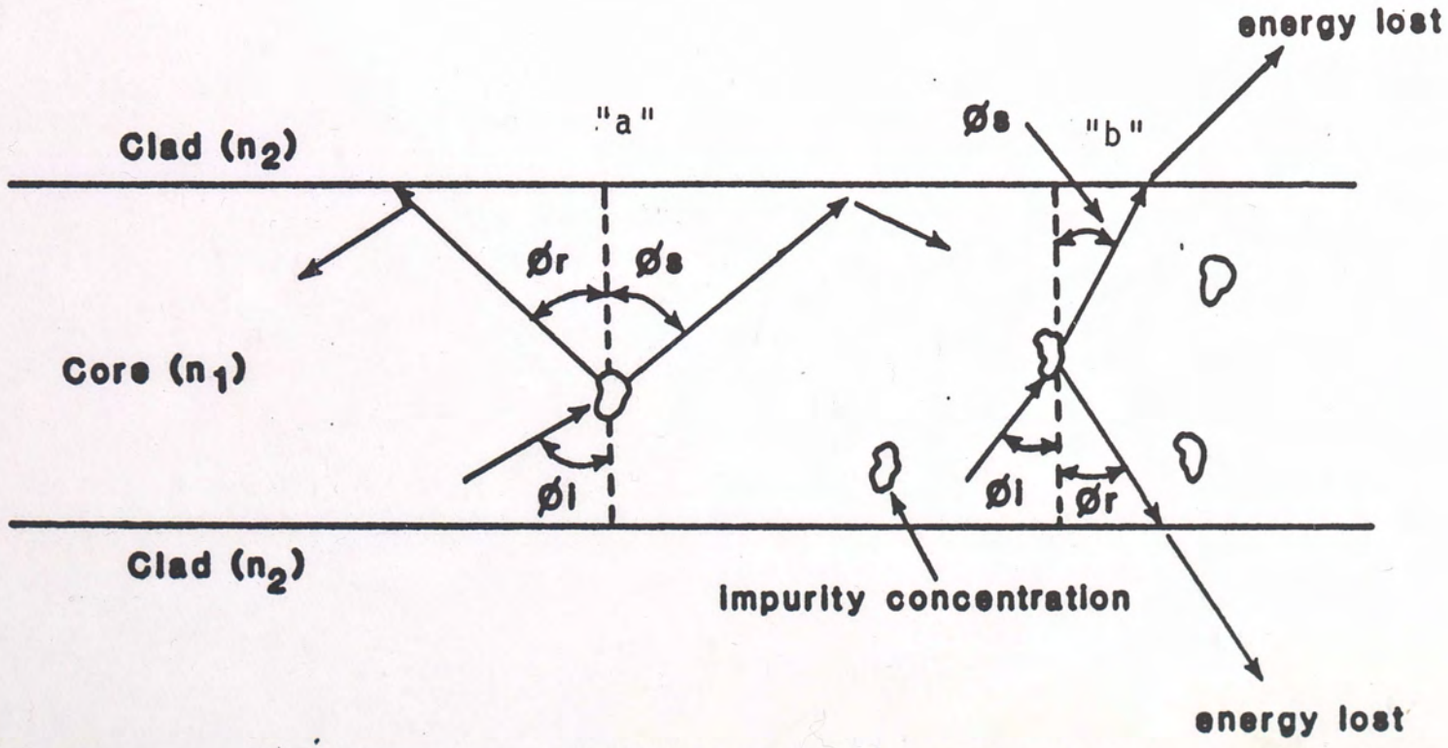

FIGURE 4-6. Scattering in an Optical Fiber Due to Impurity Concentrations.

Section 4.4: Single Mode Fiber Wavelength Cutoff Sensor

Another method of measuring temperature is to track the wavelength of the secondary mode cutoff in a single mode fiber.

Wavelength cutoff is a standard analysis technique used by the manufacturers of single mode optical fiber to determine the quality of the produced fiber. The technique is quite simple. An extremely stable broadband source is injected into a sample length of fiber (perhaps even the total length of the run). A spectrum analyzer is placed on the exit end. If the fiber is designed to be single-mode for wavelengths less than .73μm, then an abrupt increase in attenuation will occur at .73μm signifying the stripping of all higher order HE modes. This wavelength can be calculated to occur at the first zero crossing of the zeroth order Bessel function of the first kind[15] where

$$\lambda = \pi \frac{d(n_1^2 - n_2^2)^{1/2}}{2.405}$$

and d = core diameter

n_1 = core index

n_2 = clad index

Ideally, the curve as shown in Figure 10, will have a discontinuity at the cutoff. But in actuality, there will

be a slope since the fiber does not exhibit a constant numerical aperture throughout its length. This is caused by less than absolutely perfect manufacturing. But, this is not a problem as long as the slope of this curve is large enough as to not encompass the wavelength of required operation.

A temperature sensor based on this concept requires the design of an appropriate fiber which shows a significant change in core index with respect to clad index as a function of temperature. Spectrum analysis will indicate the characteristics of slope movement and thus temperature. Assuming knowledge of the fiber's characteristics, this sensor will not need recalibration even if a new instrumentation package is installed.

The data set shown in Table 4-3, was calculated using theoretical characteristics of a single mode fiber. The core index change is negligible compared with that of the clad. The clad temperature coefficient is given by

$$\frac{1}{n}\frac{dn}{dT} = 7.5 \times 10^{-5}$$

note that the index of the clad increases with temperature. This will result in less attenuation with colder temperatures for a communications system utilizing this single-mode fiber.

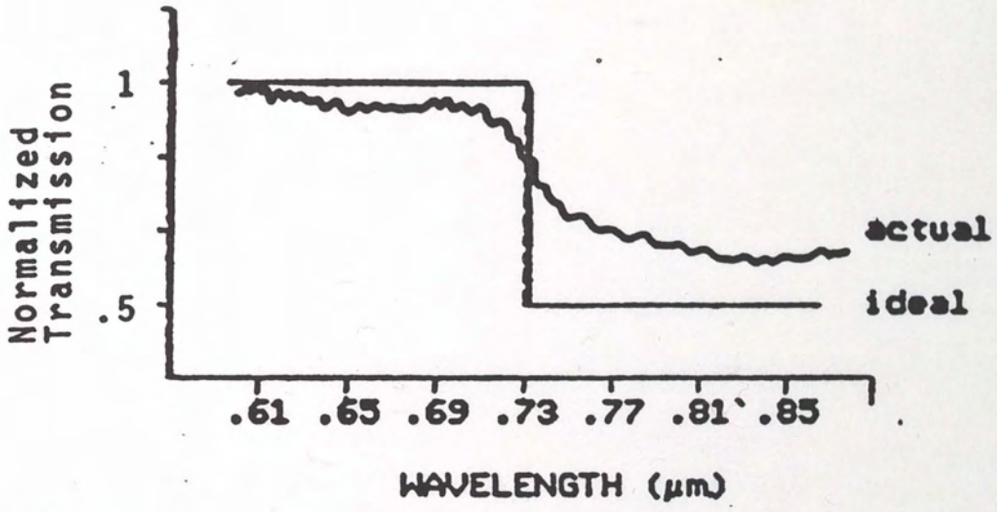

Figure 4-7. Typical SMF Cutoff Characteristics.

Source: Unpublished Data- Corning Glass Works Inc. (Corning, N.Y. 1984).

TABLE 4-3

SINGLE MODE FIBER WAVELENGTH CUTOFF SENSOR DATA

TEMP °C	CUTOFF	CHANGE IN WAVELENGTH, ANGSTROMS
0	6345.257	0
5	6297.542	-47.71533
10	6249.397	-48.14502
15	6200.944	-48.45264
20	6152.043	-49.90137
25	6102.818	-49.2251
30	6053.124	-49.69385
35	6003.224	-49.89942
40	5952.699	-50.5249
45	5901.741	-50.95801
50	5850.41	-51.33154
55	5798.544	-51.85596
60	5746.301	-52.25244
65	5693.496	-52.80518
70	5640.343	-53.15283
75	5586.611	-53.73242
80	5532.282	-54.32862
85	5477.49	-54.79248
90	5421.922	-55.49765
95	5266.074	-55.91846
100	5309.411	-56.6626
105	5252.295	-57.11621
110	5194.55	-57.74512
115	5135.996	-58.55371
120	5077.01	-58.98633
125	5017.248	-59.76221
130	4956.683	-60.56494
135	4895.284	-61.39893
140	4833.276	-62.0083
145	4770.461	-62.81446
150	4706.634	-63.82715
155	4642.195	-64.43896
160	4576.669	-65.52588
165	4510.192	-66.47754
170	4442.626	-67.56543
175	4375.206	-68.41993
180	4304.603	-69.60351
185	4233.856	-70.74707
190	4161.905	-71.9502
195	4088.589	-73.31641

CORE DIAMETER = 4.5 MICRONS
CORE BASE INDEX = 1.46
CLAD BASE INDEX = 1.456

CHAPTER 5

FIBER TEMPERATURE MEASUREMENT USING AN OPTICAL TIME DOMAIN REFLECTOMETER (OTDR) UNIT

Section 5.1: Introduction

The scattering of light energy within an optical fiber was shown in Chapter 4 to be dependent upon temperature. From this, the power attenuation of transmitted light as a function of temperature was derived for a long straight section of fiber. Measuring the transmission of light through the fiber, however, only gives the average attenuation of the whole fiber. An OTDR unit can yield the attenuation at any point along the fiber (within an instrument resolution cell). The following discussion will assess the ability of an OTDR unit to measure the temperature along any portion of the fiber by several methods.

Section 5.2: OTDR Theory

If a short pulse of light is launched into an optical fiber, some of the energy will return to the source. Before the pulse actually gets into the fiber, there are of course, Fresnel reflections off of the front surface of the fiber. This will be seen as a large spike at the detector a very

short time after the pulse is launched. For a short distance along the beginning of the guide, not all of the higher order modes have escaped; these modes enter at a higher angle to the fiber surface and hence have a higher backscatter coefficient than the steady-state propogating modes of the fiber. On the OTDR trace, this will appear as a tail on the edge of the initial spike. From then on, there is the region of linear (elastic) backscatter. This means that the backscatter is proportional to the amount of Rayleigh and Mie scattering which in turn is proportional to the actal amount of power propagating through the fiber. This leads to an exponential decay of the power in the fiber with length, as well as a resultant exponential decay of the back scattered light with time. At the end of the fiber, there is another spike, again due to Fresnel reflections off of the end surface of the fiber. This spike may be eliminated, however, by placing index matching absorbing fluid at the fiber termination.

If the group velocity of the monochromatic light pulse propogating in the fiber is C_g, we may write

$$C_g t = 2d \qquad [5\text{-}1]$$

where t is the time it takes for an impulse of light to travel from the launch point to distance d along the fiber and back again.[16] From this, we see that information about the power at any point along the fiber may be obtained from knowing how long after the pulse was launched the power was

returned. The spatial resolution of the OTDR unit is dependent upon the pulse width and the detector's speed of response. The power measurement must be averaged over a time which is significantly larger than the pulse width. If this were not so, the output signal would depend upon the pulse shape; this is undesirable since it is likely that the pulse shape will vary from one scan to another. This condition may be stated mathematically as

$$t_{av} >> t_p \qquad [5\text{-}2]$$

where t_{av} is the averaging time (and necessarily the maximum detector speed of response) and t_p is the pulse width. The minimum distance "d" which may be resolved is given by

$$d = C_g t_{av}/2 \qquad [5\text{-}3]$$

For a pulse width of 100 psec and a group velocity in the fiber of 2×10^8 m/sec we have d = 1m and $t_{av} = 10^{-9}$ sec. This is about the best resolution one can obtain with an OTDR since narrowing the pulse width and increasing the detector band width becomes very expensive and difficult.[17]

Section 5.3: Temperature Measurement Along a Fiber

For a long length of fiber wound loosely around a spool, the attenuation is given by [18]

$$a = \frac{Cn_1}{n_1 - n_2} \qquad [5\text{-}4]$$

If the fiber in question has a clad which varies with temperature as shown in Figure 4-3, then it is obvious from equation [5-4] that there will be a decrease in attenuation with an increase in temperature. We can use this change in attenuation as read by an OTDR to determine the temperature; we must make sure that the OTDR has an adequate power and range resolution to measure a defined region along the fiber. Using Figure 4-3, for example, (with n_1 = 1.45 and n_2 ranging from 1.405 at 25°C to 1.400 at 50°C), the difference in attenuation is seen to be 10% between the two temperatures. In order to resolve the temperature difference over 0.1m (the practical limit of spatial resolution for an OTDR unit), with an attenuation of 6.0 dB/Km for the fiber, the OTDR unit must be able to resolve a change of 5×10^{-5} dB or less. This implies an extremely large signal to noise ratio as well as very sensitive measurement electronics. The end result of this discussion is that this method is impractical as a line sensor; however, it may be useful in the form of a distributed point sensor as pictured in Figure 5-1. The problem with this configuration is that the sensing coils closer to the OTDR unit directly affects the apparent attenuation in the coils further down the line. This will be discussed in the next section.

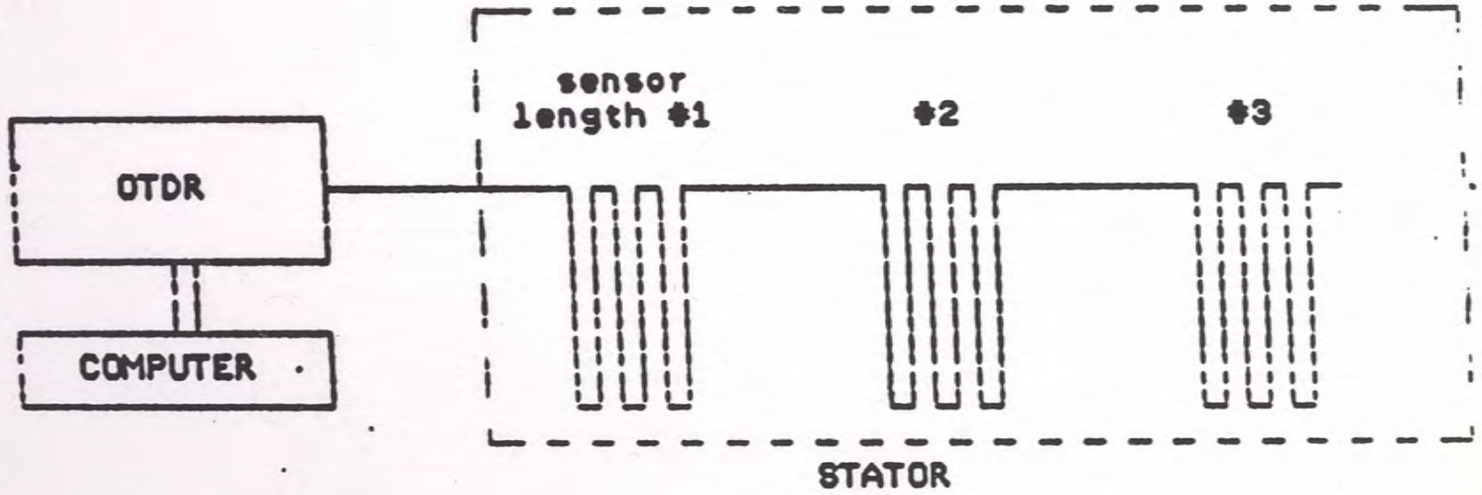

Figure 5-1. Distributed Fiber Optic Temperature Sensor.

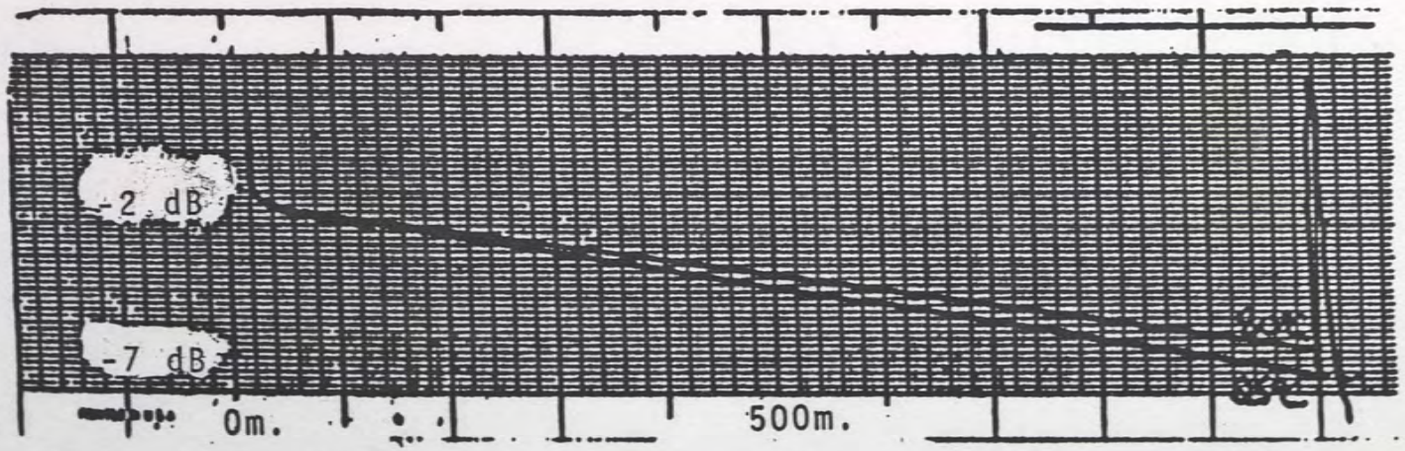

Figure 5-2. 960m. of Loosely Wound Fiber @ 25°C. and 80°C.

Section 5.4: The Effect of Temperature Upon Coiled Fiber Attenuation Characteristics

When the first section of an optical fiber is coiled around a spool of small diameter, there is an increase in attenuation for that section of fiber. Due to critical angle losses, this is expected. However the tightly wound fiber near the beginning of the OTDR line also affects the attenuation characteristics of the succeeding fiber length.

While a reference by R. Payne and L. Bouthilette (1981)[19] describes this phenomenon (for a similar situation); much of the underlying theory behind this subject has yet to be formulated. However, we may be able to derive a temperature sensor based upon empirical results provided that these results are reproducible over a period of time.

In our experimentation, we used several different coils to spool the first portion of the fiber (the portion closer to the ODTR).

Figure 5-2 shows an OTDR measurement of attenuation where a large 15" diameter spool with 960 m wound around it at 25°C and at 80°C. As mentioned in Section 4-3, there is a decrease in attenuation with temperature due to the increase in the difference between the core and clad indices. Figure 5-3 pictures the first 130m. of 960m length of fiber wound around a 6" diameter spool. The rest of the

fiber remained on the 15" diameter shipping spool. The local discontinuity where the fiber is between the two spools is evident from the figure. The smaller spool was brought to several different higher temperatures. While this only slightly increased the attenuation characteristics of the fiber on the smaller spool, it greatly increased the apparent attenuation of the fiber on the larger spool even though its temperature remained constant. It is interesting to note that the attenuation of light in the larger spool near the discontinuity is affected by the smaller spool, however, the attenuation nearer the termination of the line gradually reverts to the original value of attenuation within the large spool without the preceding smaller spool. Figures 5-2 through 5-4 show the first stretch of fiber wound around spools of various diameters. In each case, the attenuation of the larger spool (which is near the end of the line) appears to increase when the smaller (preceding) spool is heated. The smaller the diameter of the heated spool, the less fiber must be wound around it in order to obtain an apparent attenuation change in the following spool. However, the smaller diameter spool, with a long amount of fiber wound about it, will increase sensitivity (of the succeeding spools attenuation to temperature) at the expense of the signal to noise ratio. Therefore, there is a trade off between sensitivity and resolution due to the

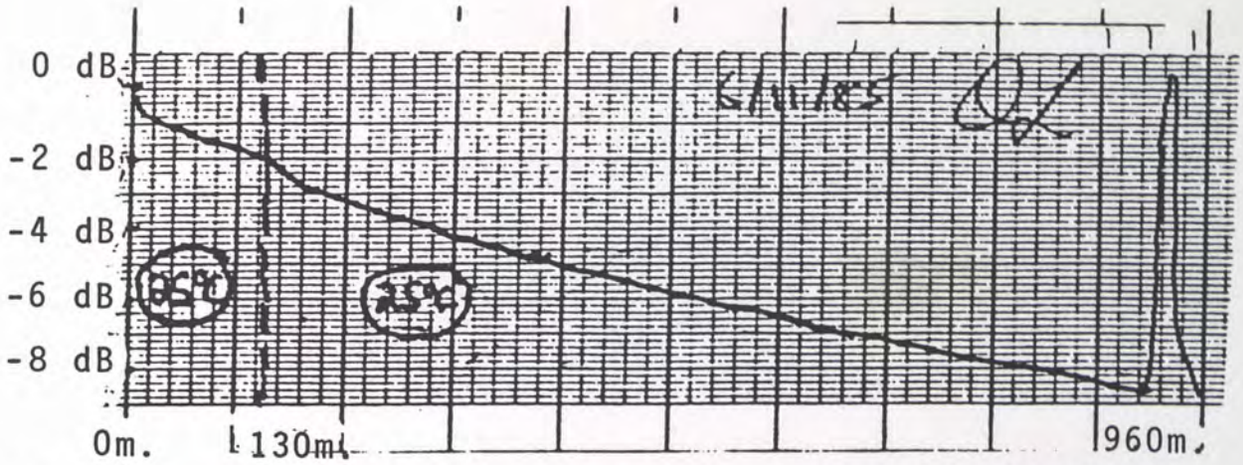

Figure 5-3(a). First 130 m. wound around 6" Diameter Spool @ 25°C.

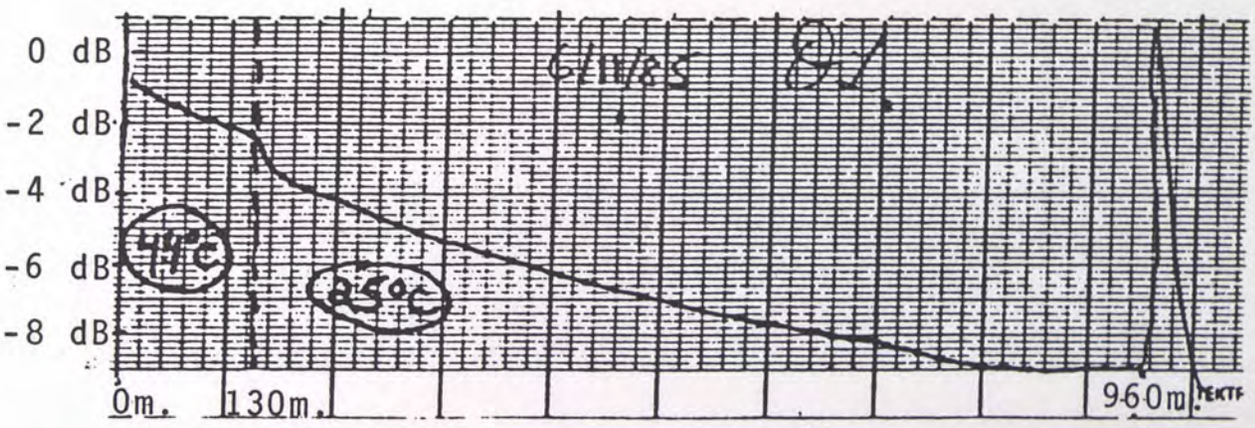

Figure 5-3(b). First 130m. wound around 6" Diameter Spool @ 44°C.

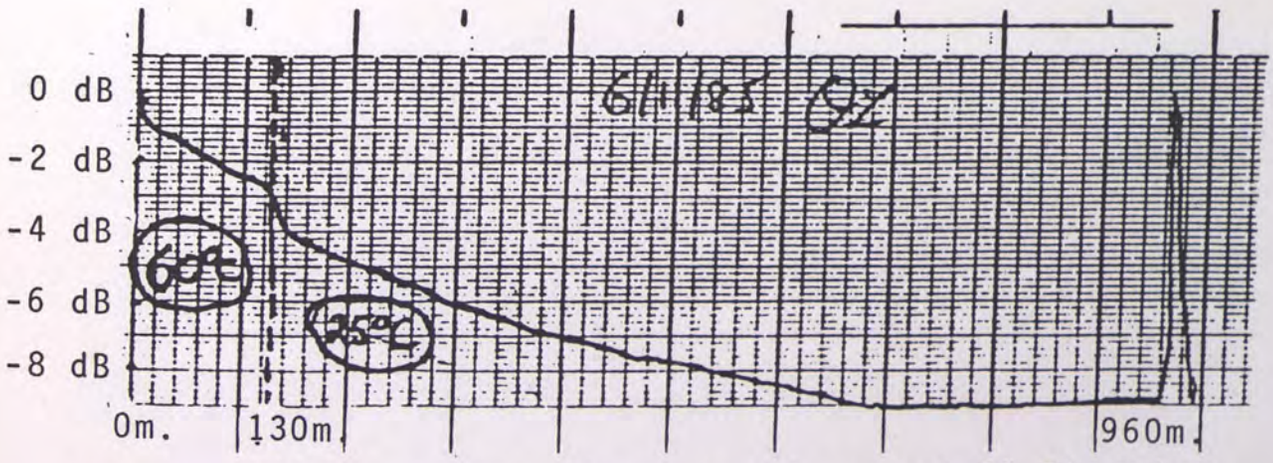

Figure 5-3(c). First 130 m. wound around 6" Diameter Spool @ 60°C.

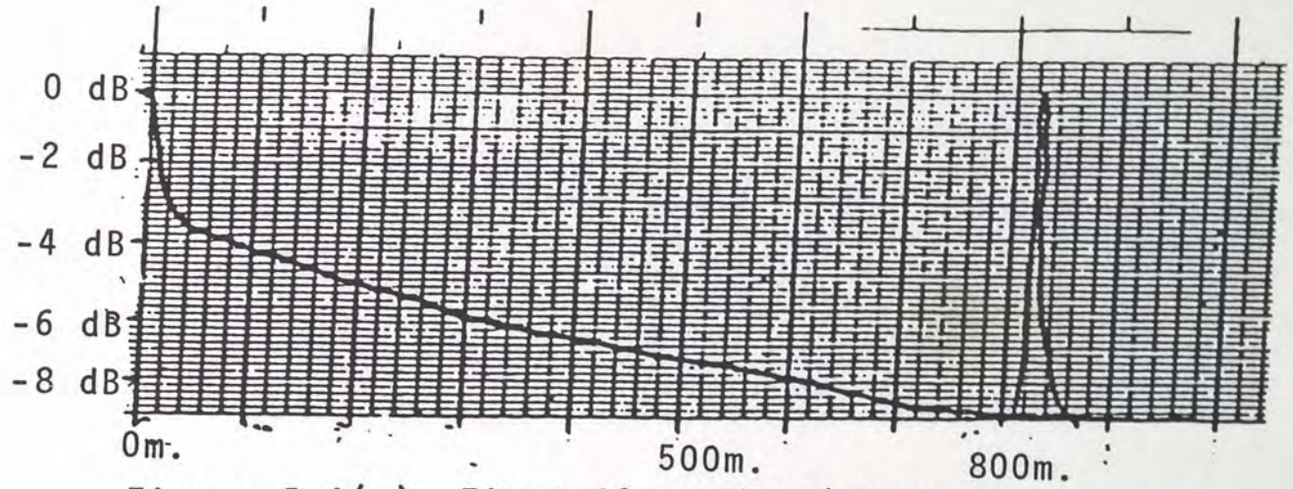

Figure 5-4(a). First 10 m. Wound Around 3" Diameter Spool @ 25°C.

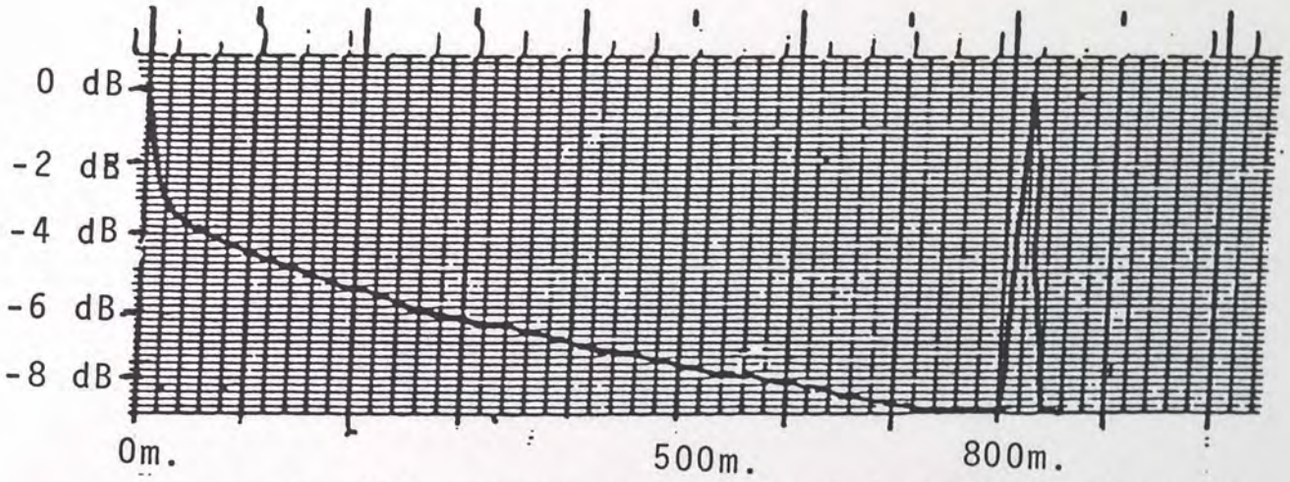

Figure 5-4(b). First 10 m. Wound Around 3" Diameter Spool @ 50°C.

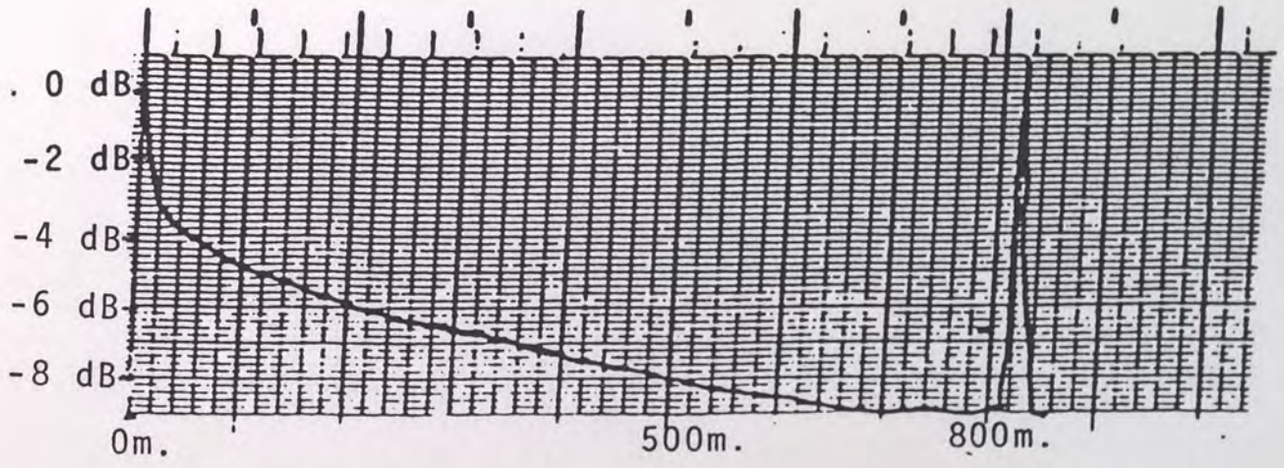

Figure 5-4(c). First 10 m. Wound Around 3" Diameter Spool @ 75°C.

degradation of the signal in a long, tightly wound length of fiber.

Section 5.5: Nonguiding Fiber Threshold Temperature Sensor

Consider an optical fiber whose core index is only slightly greater than the clad's index. Let us also assume that the core is made of a material with a more negative change in index than the clad with temperature. Once any portion of fiber rises above the temperature where the core index is reduced to the same value as that of the clad; the fiber is no longer a lightwave guide and power escapes from the core at that point. If such a fiber is attached to an OTDR unit with a resolution of .1m, then one can tell where the fiber has reached the threshold temperature (within the 10cm resolution cell). The OTDR will register a great loss of power at that point. Although this method can only detect the closest "hot spot" to the OTDR; it may be sufficient for an electric generator since the detection of any "hot spot" will require the repair of the generator.

While an OTDR does not have adequate spatial resolution to be used in a line temperature sensor with high quality resolution, it may be used in a point sensor with resolution of about 20°C or in a temperature threshold line sensor with spatial resolution between .1m and 1m as evident from Figure 5-6 (depending upon which type of ODTR one uses). It

is also possible to use the same ODTR to monitor the temperature of both multiple points and a threshold line sensor.

CHAPTER 6

CONCLUSIONS/RECOMMENDATIONS

We have evaluated several different types of fiber optic temperature sensors as candidates for monitoring the temperature along the stator windings of a large electric power generator. While the ideal sensor for this task would be a high resolution line sensor, none of these exist in present technology.

We have found however, that by measuring the spectral shift of a thin film interference filter, we may accurately determine the temperature of a single point. As discussed in Section 2.5, this technique does lend itself to permanent calibration. The narrow band light source transmission through a thin film filter is also a measurable function of temperature; however, its use in a temperature sensor is limited since the transmission characteristics of the guiding fibers will vary with temperature as well as aging. This will not matter in the spectral shift sensor as long as we assume that the normalized fiber transmission spectrum remains constant under all conditions. This is a reasonable assumption.

Interferometric temperature sensors are very sensitive to external vibrations. Also, the single mode fiber (which must be used in an interferometer) is very fragile. Under

the rough conditions inside the generator an interferometric sensor would be extremely difficult to maintain.

We have shown that an OTDR does not have adequate spatial resolution (or attenuation resolution) to measure the temperature at many different points along a relatively short (10m) strand of fiber which will be placed among the stator sindings of the generator. By coiling a short length of a spool of fiber around a small diameter spool and then monitoring the attenuation of optical power in the fiber left on the shipping spool as the smaller spool is heated, we may obtain a point sensor with a temperature resolution of about 20°C. Since there are other point temperature sensors which have much better resolution (such as the thin film interference filter), OTDR systems shall not be used as point sensors (at least not in sensors based upon apparent attenuation).

In order to completely monitor the temperature distribution within a generator, one must have multiple high resolution point sensors as well as a threshold line sensor with a resolution of less than 1 meter. The most effective combination of sensors which meet these requirements is the filter spectrum shift sensor (see Section 2.5) used in conjunction with the nonguiding fiber/ODTR technique (see Section 5.5). The filter sensors may be wavelength multiplexed. This will allow multiple sensors to be analyzed by one spectral scan. A spectrometer may seem

expensive, however, by a combination of time and wavelength, multiplexing many points may be measured thus reducing the cost per point. The nonguiding fiber may be used with only a light source and a detector (rather than an OTDR), however, despite the cost savings, this will not tell where along the stator runs the threshold temperature has been reached.

Until now, we have assumed that magneto-optic effects are negligible. While this premise is backed up by measured results,[20] we must install a test sensor inside a generator (or a simulator of generator conditions) in order to determine if a temperature sensitive material will be effected by the magnetic fields (and other conditions within the generator).

APPENDIX

SPECTROMETER CONTROL SOFTWARE

```
100 INIT
110 DIM B(100),C(100),D(100),E(100),F(100),G(100),H(100),J(100)
120 DIM L(100)
130 ON SRQ THEN 140
140 PRINT @7;"REN;"
150 FOR I=1 TO 300
160 NEXT I
170 GO TO 200
180 PRINT @7;"LE1;"
190 PRINT @7;"TE3;"
200 PRINT @7;"C;"
210 FOR I=1 TO 200
220 NEXT I
230 PRINT @7;"A 836 50 1546 8289 0;"
240 PRINT @7;"H;"
250 PRINT @7;"O 4 0;"
260 INPUT @7:M,N,O,P,Q,R,S,T,U
270 Y=0
280 X=0
290 Z=0
300 FOR A=1 TO 63
310 INPUT @7;B(A),C(A),D(A),E(A),F(A),G(A),H(A),J(A),L(A)
320 IF A<7 THEN 370
330 IF A>10 THEN 370
340 Y=B(A)*C(A)+(B(A)+1)*D(A)+(B(A)+2)*E(A)+(B(A)+3)*F(A)+Y
350 Y=Y+(B(A)+4)*G(A)+(B(A)+5)*H(A)+(B(A)+6)*J(A)+(B(A)+7)*L(A)
360 X=X+C(A)+D(A)+E(A)+F(A)+G(A)+H(A)+J(A)+L(A)
370 NEXT A
380 INPUT @7;Z$,Y$
390 Z=Y/X
400 PRINT "THE AVERAGE BUG POSITION IS  ";Z
410 B(67)=6*(Z-72)+5774
420 PRINT "THE AVERAGE WAVELENGTH IS  ";B(67);"  ANGSTROMS."
430 B(68)=(Z-71.53)/0.03
440 B(68)=B(68)+45
450 B(68)=INT(B(68))
460 PRINT
470 Q$="                                                    "
480 PRINT Q$,B(68);" DEG C."
490 B(69)=INT(B(68)*9/5)+32
500 PRINT Q$,B(69);" DEG F."
510 GO TO 200
520 END
```

END NOTES

[1]Yariv, A., Introduction to Optical Electronics. (New York: Holt, Rinehart and Winston, 1976), p. 60.

[2]Saff, E.B., Fundamentals of Complex Analysis. (New Jersey: Prentice-Hall, 1976), p. 172.

[3]Infared Industries Incorporated, The Spectrum of IR Filters. (Orlando, FL, 1984) p. 6.

[4]Born, M. and Wolf, E., Principals of Optics. (Oxford, England: Pergamon Press, 1980), p. 347.

[5]Hoya Corporation, Hoya Optical Glass Catalog No. 8008. (Fremont, CA, 1980) pp. 29-83.

[6]Lagakos, N. and Bucaro, J., "Minimizing temperature sensitivity of optical fibers," Applied Optics, 20, (1981):3277.

[7]Corion Corporation, Optical Filters and Coatings. (Holliston, Mass., 1983) pp. 19031.

[8]Dereniak, E. L. and Crowe, D.G.. Optical Radiation Detectors, (New York: Wiley, 1984), pp. 135-36.

[9]Cherin, A., An Introduction to Optical Fibers (New York: McGraw-Hill, 1983), p. 93.

[10]Lagakos, N. and Bucaro, J., "Minimizing temperature sensitivity of optical fibers," Applied Optics, 20, (1981):3277.

[11]Ibid.

[12]Cherin, A., An Introduction to Optical Fibers (New York: McGraw-Hill, 1983), p. 93.

[13]Barnoski, Michael, Fundamentals of Optical Fiber Communication. (New York: Academic Press, 1976), p. 29.

[14]Ibid.

[15]Cherin, Introduction to Optical Fibers, p. 94.

[16]Rogers, A.J., "Polarization Optical Time Domain Reflectometry," Applied Optics, 20, (1981):1061.

[17]Ibid.

[18]Barnoski, Optical Fiber Communications, p. 51.

[19]Payne, R. and Bouthilette, L., "OTDR study of temperature effects in optical cables," 3rd Intl. Conf. on Optical Fiber Communications. (San Diego, CA, 1981), MA4.

[20]Amnon Yariv and Pochi Yeh, Optical Waves in Crystals. (New York: Wiley, 1984) p. 103.